5-Aminolevulinic Acid Dehydratase Gene Dosage Affects Programmed Cell Death and Immunity[1]

Qichao Chai,[a,2] Xiaoguang Shang,[a,2] Shuang Wu,[a] Guozhong Zhu,[a] Chaoze Cheng,[a] Caiping Cai,[a] Xinyu Wang,[b,3] and Wangzhen Guo[a,3]

[a]State Key Laboratory of Crop Genetics and Germplasm Enhancement, Cotton Hybrid R & D Engineering Center (the Ministry of Education), Nanjing Agricultural University, Nanjing 210095, China
[b]College of Life Sciences, Nanjing Agricultural University, Nanjing 210095, China

ORCID IDs: 0000-0002-8458-9590 (C.Ch.); 0000-0003-3333-7147 (W.G.).

Programmed cell death (PCD) is an important form to protect plants from pathogen attack. However, plants must precisely control the PCD process under microbe attacks to avoid detrimental effects. The complexity of how plants balance the defense activation and PCD requires further clarification. Lesion mimic mutants constitute an excellent material to study the crosstalk between them. Here, we identified a *Gossypium hirsutum* (cotton) lesion mimic mutant (*Ghlmm*), which exhibits necrotic leaf damage and enhanced disease resistance. Map-based cloning demonstrated that *GhLMMD*, encoding 5-aminolevulinic acid dehydratase and located on chromosome D5, was responsible for the phenotype. The mutant was resulted from a nonsense mutation within the coding region of *GhLMMD*. It exhibited an overaccumulation of the 5-aminolevulinic acid, elevated levels of reactive oxygen species and salicylic acid, along with constitutive expression of pathogenesis-related genes and enhanced resistance to the *Verticillium dahliae* infection. Interestingly, *GhLMM* plays a dosage-dependent role in regulating PCD of cotton leaves and resistance to *V. dahliae* infection. This study provides a new strategy on the modulation of plant immunity, particularly in polyploidy plants.

Cell death in plants can occur as part of normal developmental processes, which is traditionally considered to be a programmed cell death (PCD) process, or ectopically when the normal development is perturbed, such as by a genetic lesion. In addition, cell death can occur at the sites of environmental stresses, such as pathogen infection or physical wounding, or in response to low concentrations of toxins. These three distinct types of cell death—in normal development, in perturbed development, or because of environmental stresses—do not necessarily utilize the same cell death mechanism; however, they do all appear to occur via a controlled disassembly of the cell (Vaux and Korsmeyer, 1999; Pennell and Lamb, 1997).

In plants, the hypersensitive response (HR), which results in cell death at the sites of infection by an avirulent pathogen, has received considerable attention in the study of PCD and its relationship to plant disease resistance (Heath, 2000). Cell death during HR is elicited by specific recognition of pathogen-derived molecules from avirulent pathogens by plant proteins encoded by resistance (R) genes. The recognition is followed by local accumulation of reactive oxygen species (ROS), salicylic acid (SA), and defense-related proteins such as pathogenesis-related (PR) proteins, and is accompanied by the production of antimicrobial molecules and the fortification of cell walls (Shirasu and Schulze-Lefert, 2000). Considerable efforts have been made to identify the signaling components involved in the HR control and their connection to disease resistance. One approach is to identify mutants that fail to develop HR and resistance in response to infection by normally avirulent pathogens. Many of these mutations are involved in R-genes and R-protein signaling components. The second approach is to identify mutants that develop HR-like lesions and activate defense responses in the absence of pathogens. These mutants are collectively designated as lesion mimic mutants or lesion mimics, based on their spontaneous development of lesion phenotypes akin to HR or disease symptoms (Brodersen et al., 2002).

Several lesion mimic mutants have been reported in model plant Arabidopsis (*Arabidopsis thaliana*; Ishikawa

[1] This work was supported by National Key R & D Program for Crop Breeding (2016YFD0100306), and Jiangsu Collaborative Innovation Center for Modern Crop Production project (No.10). The funders had no role in study design, data collection and analysis, decision to publish, or preparation of the manuscript.

[2] These authors contributed equally to the article.

[3] Address correspondence to Wangzhen Guo (moelab@njau.edu.cn) and Xinyu Wang (xywang@njau.edu.cn).

The author responsible for distribution of materials integral to the findings presented in this article in accordance with the policy described in the Instructions for Authors (www.plantphysiol.org) is: Wangzhen Guo (moelab@njau.edu.cn). W.G. and X.W. conceived this project; W.G., X.W, Q.C., and X.S. designed all experiments; Q.C. and X.S. performed the experiments and analyzed the data under the supervision of W.G. and X.W., with assistance from S.W and C.Ca. for map based cloning, and G.Z. and C.Ch for RNA-seq analysis; W.G., X.W., X.S., and Q.C. wrote the manuscript; W.G. and X.W. revised the manuscript.

www.plantphysiol.org/cgi/doi/10.1104/pp.17.00816

et al., 2001; Quesada et al., 2013) as well as in cultivated crops such as maize (*Zea mays*; Hu et al., 1998), rice (*Oryza sativa*; Sun et al., 2011), and wheat (*Triticum aestivum*; Wang et al., 2016). Among them, about 40 genes controlling the lesion mimics have been isolated (Bruggeman et al., 2015). The proteins encoded by these genes fall into various functional groups, including membrane associated protein (Büschges et al., 1997), ion channel (Balagué et al., 2003), zinc-finger protein (Dietrich et al., 1997), and components involved in the biosynthesis/metabolic pathways of fatty acid/lipids (Kachroo et al., 2001) and porphyrin (Hu et al., 1998). Porphyrin compounds such as chlorophyll and heme play vital roles in plant development. The misregulation of chlorophyll metabolism can lead to severe photooxidative stress, resulting in cell damage, cell death, or ultimately plant death. In Arabidopsis, lesion mimic mutants *lin2* and *rug1* were related to the loss of function of coproporphyrinogen III oxidase (CPO) and porphobilinogen deaminase, respectively (Ishikawa et al., 2001; Quesada et al., 2013). Likewise, disruption of CPO in rice lesion initiation 1 mutant leads to cell death phenotypes (Sun et al., 2011). Interestingly, enzymes in chlorophyll biosynthesis or degradation have also been linked to system acquired resistance (SAR). Down-regulation of urophorphyrinogen decarboxylase III or CPO in tobacco (*Nicotiana tabacum*) and protoporphyrinogen oxidase in Arabidopsis would lead to lesions on the leaves, accompanied by the constitutive expression of PR genes, high levels of SA accumulation, and increased resistance to pathogens (Mock and Grimm, 1997; Kruse et al., 1995; Molina et al., 1999). In addition, the light signaling factors FHY3 and FAR1 could regulate plant PCD and disease immunity by modulating chlorophyll biosynthesis (Tang et al., 2012; Wang et al., 2015). Despite these advances, the molecular mechanisms by which homeostatic disruption of chlorophyll metabolism could induce PCD and SAR in plant remain elusive.

The allotetraploid Upland cotton (*Gossypium hirsutum*) accounts for more than 90% of the world's cotton production, providing an important source of renewable textile fibers and oilseeds. Compared with the other widely cultivated crops such as maize, rice, and wheat, no lesion mimic mutants are discovered in cotton. In the photosynthesis biological process, 5-aminolevulinic acid dehydratase (ALAD) is an enzyme that functions at an early step in chlorophyll and heme biosynthesis. To our knowledge, no *ALAD* mutants have been reported in any plants. Here, we report the identification and characterization of a cotton lesion mimic mutant. Map-based cloning revealed that the mutant was developed from a premature mutation within the *GhLMMD* gene that encodes ALAD. The mutant exhibits high levels of aminolevulinic acid (ALA), ROS, and SA, constitutive expression of PR genes, and enhanced resistance to *Verticillium dahliae* infection. Remarkably, reduced ALAD enzyme activity is proportional to the increased levels of *PR* gene expressions and the degree of PCD. Similarly, the copy number of the mutant *GhLMM* was positively related to the severity of PCD, the levels of ROS, SA, and PR gene expressions, and the level of resistance to *V. dahliae* infection. We propose that *ALAD* plays a dosage-dependent role in the regulation of PCD and immunity in allotetraploid cotton and potentially other polyploidy plants, which might have practical significance in breeding crops with improved resistance to pathogens.

RESULTS

Genetic and Physical Mapping of the *GhLMMD* Locus

In a screen for the transgenic plants of cotton, we discovered a natural variation seedling that shows disease-like cell death phenotype during its development in the absence of pathogens. A subsequent analysis revealed that no T-DNA insertion was present in the plant, suggesting that it might originate from a mutation in the tissue culture process. We named the mutant *Ghlmm* (*Gossypium hirsutum* lesion mimic mutant). *Ghlmm* shows necrotic lesions only on the leaves but not in other tissues of the cotton plant (Fig. 1A). Further phenotypic investigation demonstrated that *Ghlmm* develops lesions in a temperature- and light-dependent manner. Under higher temperatures of 28/24°C (day/night) and long-day conditions of 16 h/8 h (light/dark), the mutant impaired leaf development and formed lesions. However, under the lower temperatures of 23/20°C (day/night) or short-day conditions of 8 h/16 h (light/dark), the leaf lesions did not appear (Supplemental Fig. S1). Though exhibiting a lesion mimic phenotype on the leaves under field conditions, other traits, such as fiber yield and quality and seed development, were almost not affected in *Ghlmm* compared with its corresponding wild-type accession W0 (Supplemental Table S1).

To better understand the molecular basis of the lesion mimic phenotype identified in cotton, we employed a map-based cloning strategy to isolate the target gene. As a first step to clone the gene, we initiated a genetic and physical mapping program to delimit the gene locus. The F_1 and F_2 mapping populations were developed by crossing *Ghlmm* with TM-1, a genetic standard line of *G. hirsutum*. All F_1 plants exhibit the wild-type phenotype, and the segregation of the F_2 plants meets the Mendelian ratio of 3:1 (554 individuals with wild-type phenotype and 209 individuals with lesion mimic phenotype, $\chi^2 = 2.202 < \chi^2_{0.05,1} = 3.84$), suggesting that the lesion mimic phenotype was controlled by a single nuclear recessive gene. Linkage analysis with 763 F_2 plants delimited the target gene to a 371-kb DNA segment by markers NAU7928 (microsatellite) and S2393 (single nucleotide polymorphism [SNP]) on Chr. D5 (Fig. 1B), we therefore named the target gene *GhLMMD*. According to the high-quality reference genome sequence of the tetraploid cotton *G. hirsutum* acc. TM-1 (Zhang et al., 2015), the 371-kb region contains 25 open reading frames. The transcriptome analysis in TM-1 revealed that there are 12 genes whose FPKM

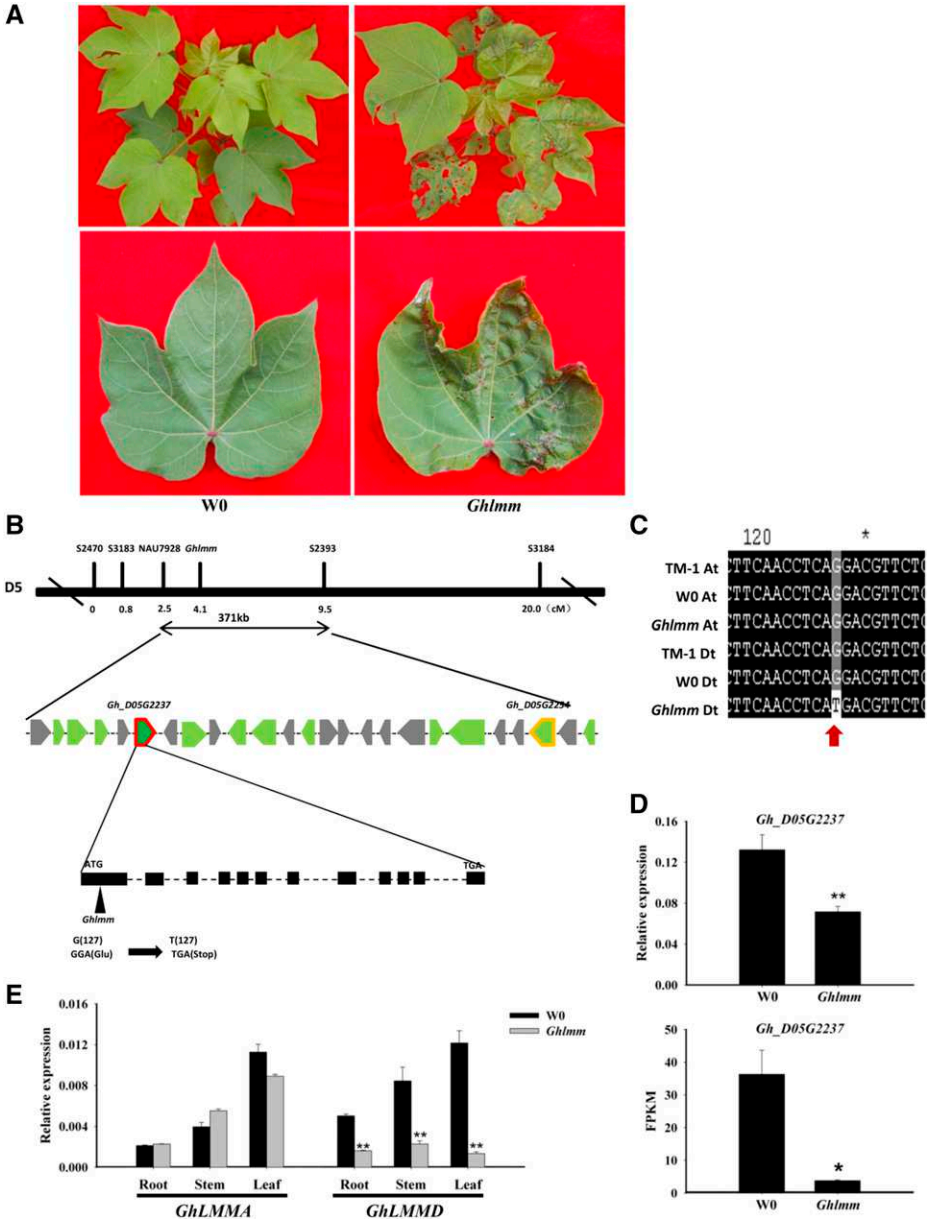

Figure 1. Lesion phenotype of *Ghlmm* mutant and physical delineation of *GhLMMD*. A, Phenotypes of 3-month-old wild type (WT) and *Ghlmm* plants grown in the field. The *Ghlmm* mutant exhibits spontaneous disease like lesions on the leaves. B, Physical map of the *GhLMMD* locus. *GhLMMD* was delimited to a 371-kb region on Chromosome D5. Vertical lines mark the positions of DNA markers flanking *GhLMMD*. Twenty-five genes (denoted by gray and green thick arrows) were predicted within the region, among which 12 (green thick arrows) were verified to be active genes based on RNA-seq data and qRT-PCR analysis. The expression of two of these genes, termed *Gh_D05G2237* and *Gh_D05G2254*, were significantly decreased in *Ghlmm* mutant and might be the candidates of *GhLMMD*. C, DNA sequence comparisons of the candidate genes, between the mutant and the wild type, identified a point mutation (G-to-T transition at the 127th position from the start codon, marked with a red thick arrow) in *Gh_D05G2237* on Chromosome D5. D, Transcript abundance of *Gh_D05G2237* in the mutant and the wild type analyzed by qRT-PCR and RNA-seq. Data were obtained from three independent replicates. E, Expression of *GhLMMA* and *GhLMMD* in different tissues in the mutant and the wild type, showing that transcript abundance of *GhLMMA* was not altered in both the mutant and the wild type, while the transcript abundance of *GhLMMD* was remarkably decreased in the mutant but not in wild type, further demonstrating that the mutation has taken place in the D genome. $^{*}P < 0.05$ and $^{**}P < 0.01$ respectively (Student's *t* test). Error bars are SE of three biological replicates.

value was >1.0 (Supplemental Fig. S2A), suggesting that they are probably active genes. The expressions of these genes were further detected by quantitative RT-PCR (qRT-PCR). It was found that among them, two genes, named *Gh_D05G2237* and *Gh_D05G2254*, were significantly decreased in transcript abundance in *Ghlmm* mutant compared with that in W0 (Supplemental Fig. S2B). Therefore, the two genes were considered as the candidate gene for *GhLMMD*.

Identification of *GhLMMD*

To identify *GhLMMD*, the DNA and cDNA of *Gh_D05G2237* and *Gh_D05G2254* in *Ghlmm*, W0, and TM-1 were respectively amplified and sequenced. Sequence comparisons showed that no nucleotide differences in *Gh_D05G2254* were detected in *Ghlmm*. However, a point mutation (G-to-T transition at the 127th position within the coding region) was detected in *Gh_D05G2237* of *Ghlmm* compared with that of W0 and TM-1 (Fig. 1C), which resulted in a pretermination (GGA to TGA) in the protein. Next, we tested whether silencing *Gh_D05G2237* or *Gh_D05G2254* would result in the lesion mimic phenotype. They are suppressed in the wild-type cotton seedlings by the TRV-based virus-induced gene silencing (VIGS) technology, respectively. Suppression of *Gh_D05G2237*, but not *Gh_D05G2254*, led to a lesion mimic phenotype on the leaves (Supplemental Figs. S3 and S4). To further verify whether *Gh_D05G2237* is the candidate of *GhLMMD*, qRT-PCR and a transcriptome analysis were performed for *Ghlmm* and W0.

The results showed that the transcript abundance of *Gh_D05G2237* was indeed drastically decreased in *Ghlmm* (Fig. 1D). Based on the point mutation that occurred at the 127th position within the coding region of *Gh_D05G2237*, SNP primers that could specifically detect the 127th-T genotype but not the 127th-G were developed and successfully used in genotyping 209 F_2 plants exhibiting the *Ghlmm* phenotype.

Since upland cotton is an allotetraploid plant, it consists of the A and D subgenome. To confirm that *Ghlmm* was caused by a mutation in *GhLMMD* but not in *GhLMMA*, the *GhLMMD* homologs in the A subgenome and transcript abundance of *GhLMMD* and *GhLMMA* were respectively monitored by qRT-PCR using gene-specific primers (designed based on other SNP sites between *GhLMMA* and *GhLMMD* rather than the pretermination site in *GhLMMD*; Supplemental Table S2). It was shown that the transcript abundance of *GhLMMD* was indeed decreased in *Ghlmm* compared with W0, whereas the *GhLMMA* expression was not significantly altered in *Ghlmm* and W0 (Fig. 1E). These experiments indicate that the mutation leading to the lesion mimic phenotype occurred in the D subgenome and that *Gh_D05G2237* is the target gene of *GhLMMD*.

GhLMMD Encodes the ALA Dehydratase and Localizes in Chloroplasts

The BLAST analysis using *Gh_D05G2237* as query showed that *GhLMMD* encodes a predicted protein of 430 amino acid residues with a conserved ALAD motif (Pfam00490) in the region from amino acid 105 to 424, with an 84% similarity to the reported AtHEMB1 protein in Arabidopsis (Supplemental Fig. S5). A nonsense mutation occurred in *GhLMMD* at the 43rd amino acid leads to a predicted truncated protein in *Ghlmm*. Wild-type *GhLMMD* and its corresponding gene in the A subgenome, *GhLMMA*, are highly conserved in the amino acid sequence (99% identity) and show similar expression patterns in all tested cotton tissues, with higher expression levels in leaves, early stage ovules, and developing fibers (Fig. 2A). The phylogenetic analysis with 23 *GhLMM* orthologs (temporally named *ALAD* genes here) derived from 17 species, including algae, fern, moss, gymnosperms, monocotyledons, and dicotyledons (Supplemental Table S3) revealed that no more than two *ALAD* genes was found in each tested species (Fig. 2B) and the ALAD motifs share high sequence similarities, indicating that ALAD is an ancient and conserved protein in plants (Fig. 2B). The subcellular localization showed that both GhLMMA and GhLMMD proteins localize in chloroplasts (Fig. 2C), which is consistent with their function in the tetrapyrrole biosynthesis pathway.

Reduced ALAD Activity Leads to Elevated Levels of ALA, ROS, and MDA

In plants, ALAD is an enzyme at an early step in the tetrapyrrole biosynthesis pathway, catalyzing the porphobilinogen (PBG) formation by condensing two molecules of the ALA. To reveal how the *GhLMMD* mutation affects ALAD activity, we expressed the wild-type GhLMMD protein and the corresponding mutant protein in *Escherichia coli* and measured their catalytic activities in vitro after purification. The wild-type GhLMMD protein was successfully expressed and purified (Fig. 3A, lanes 2 and 3), whereas the mutant protein could not (Fig. 3B, lanes 2 and 3). Western blotting using anti-His antibody further showed the purified wild-type GhLMMD protein, while no mutant protein was obtained (Fig. 3C). It is possible that the preterminated *GhLMMD* in *Ghlmm* could not be translated or the truncated protein (only 42 amino acids) was degraded in *E. coli*. Compared to the high enzyme activity of purified GhLMMD protein, the activity of mutant protein was undetectable (Fig. 3D).

In vivo, *GhLMMD* mutation might reduce the ALAD enzyme activity and result in overaccumulation of its substrate ALA and decreased levels of PBG. In line with our hypothesis, the enzyme activity of ALAD in the leaves of *Ghlmm* decreased by 28.5% (Fig. 3E), the PBG content decreased by about 29.7% (Fig. 3F), but the ALA content increased by 1.5-fold (Fig. 3G) in *Ghlmm* compared to W0.

Previous studies have shown that the ALA accumulation could generate reactive oxygen species from autoxidation and photochemical reactions (Ryter and Tyrrell, 2000). Thus, overaccumulation of ALA would produce excessive amounts of ROS in the *Ghlmm* leaves. Indeed, H_2DCFDA and 3,3′-diaminobenzidine (DAB) staining demonstrated that the ROS levels were remarkably higher in mutant leaves than in wild-type leaves (Fig. 3, H and I). The measurement of the H_2O_2 content showed it is about 50% higher in mutant leaves than in wild-type leaves (Fig. 3J). ROS-related oxidation can cause plasma membrane damage by oxidizing the polyunsaturated fatty acids in the cells, ultimately resulting in cell death (Torres et al., 2006). The methane dicarboxylic aldehyde (MDA) production is an indication of the peroxidation of unsaturated membrane lipids in cells. Measurement of the MDA content showed that its level is about 72% higher in mutant leaves than in wild-type leaves (Fig. 3K).

Due to the high sequence similarity between *GhLMMA* and *GhLMMD*, TRV-based VIGS of *GhLMM* in the wild type would simultaneously suppress the expression of both of the genes and result in more severe phenotype and overaccumulation of ALA, H_2O_2, and MDA. To confirm this, *GhLMM*-silenced wild-type W0 plants were investigated at the phenotypic and molecular level. We observed that severe necrotic lesions developed in the new emerging leaves of the *GhLMM*-silenced cotton plants at 10 d after infiltration, and, notably, the leaf growth of the *GhLMM*-silenced plants was arrested and no new leaves grew out after the emergence of the first true leaf (Supplemental Fig. S4A). As expected, the expression of both *GhLMMA* and *GhLMMD* was drastically decreased (Supplemental Fig. S4B), and

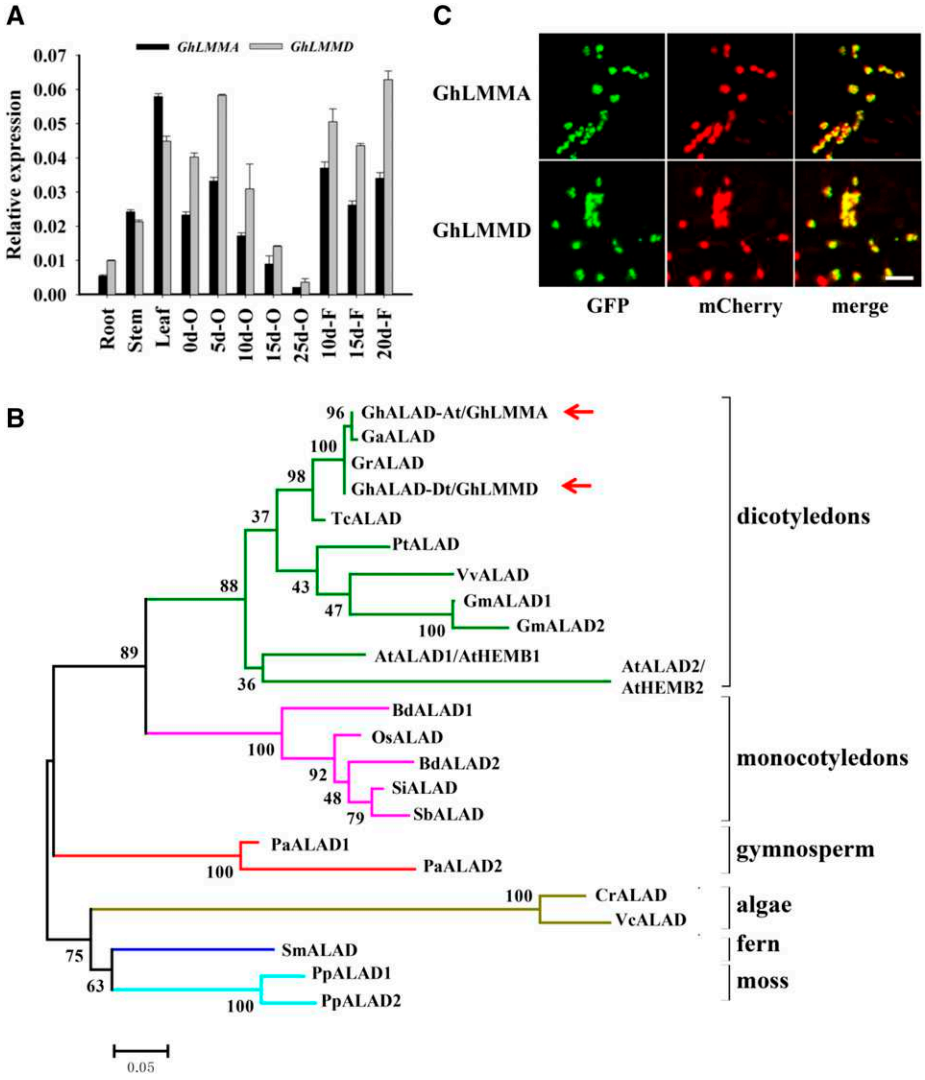

Figure 2. Characterization of *GhLMMD*. A, Transcript abundance of *GhLMMA* (*GhLMM* in A subgenome) and *GhLMMD* (*GhLMM* in D subgenome) in different tissues of *G. hirsutum* acc. TM-1 quantified by qRT-PCR using gene-specific primers. *GhLMMA* and *GhLMMD* showed similar expressions in tested cotton tissues, with higher expression levels in leaves, early stage ovules, and developmental fibers. B, Phylogenetic analysis of the *GhLMM* orthologs (*ALAD* genes) in different species. Twenty-three ALAD proteins from 17 species, including algae, ferns, moss, gymnosperms, and angiosperms, were used to construct the phylogenetic tree. Species analyzed included algae (*Cr*: *Chlamydomonas reinhardtii*; *Vc*: *Volvox carteri*), fern (*Sm*: *Selaginella moellendorffii*), moss (*Pp*: *Physcomitrella patens*), gymnosperm (*Pa*: *Picea abies*), monocotyledons (*Si*: *Setaria italic*; *Sb*: *Sorghum bicolor*; *Bd*: *Brachypodium distachyon*; *Os*: *Oryza sativa*), and dicotyledons (*Tc*: *Theobroma cacao*; *Gh*: *Gossypium hirsutum*; *Gr*: *Gossypium raimondii*; *Ga*: *Gossypium arboreum*; *At: Arabidopsis thaliana*; *Pt*: *Populus trichocarpa*; *Vv*: *Vitis vinifera*; *Gm*: *Glycine max*). Red arrows indicate GhLMMA and GhLMMD. C, Chloroplast localization of GhLMM. GhLMMA and GhLMMD were respectively fused with GFP and transiently expressed in tobacco epidermal cells by *Agro*-infiltration. Chloroplast localized Rubisco protein fused with mCherry was used as positive control. GhLMM-GFP fusion proteins colocalize with Rubisco-mCherry fusion and show yellow signals after merging. Bars = 20 μm.

ALA, H_2O_2, and MDA were overproduced in the *GhLMM*-silenced cotton plants more than in the mock-treated W0 plants (Supplemental Fig. S4C). In a parallel experiment, the ALAD enzyme activity was inhibited by spraying 20 mM levulinic acid (LA), a specific inhibitor of ALAD, on the leaves of wild-type plants. The results showed that a similar necrotic lesion phenotype could appear on the leaves of the wild-type plants as on the leaves of the *GhLMM*-silenced wild-type plants (Supplemental Fig. S6A). Meanwhile, the levels of ALA and H_2O_2 had increased 2.7- and 2.5-fold, respectively, in LA-treated leaves, compared with the mock-treated leaves (Supplemental Fig. S6, B and C). This experiment demonstrated that *GhLMM* silencing has the same effects as the ALAD enzyme disruption.

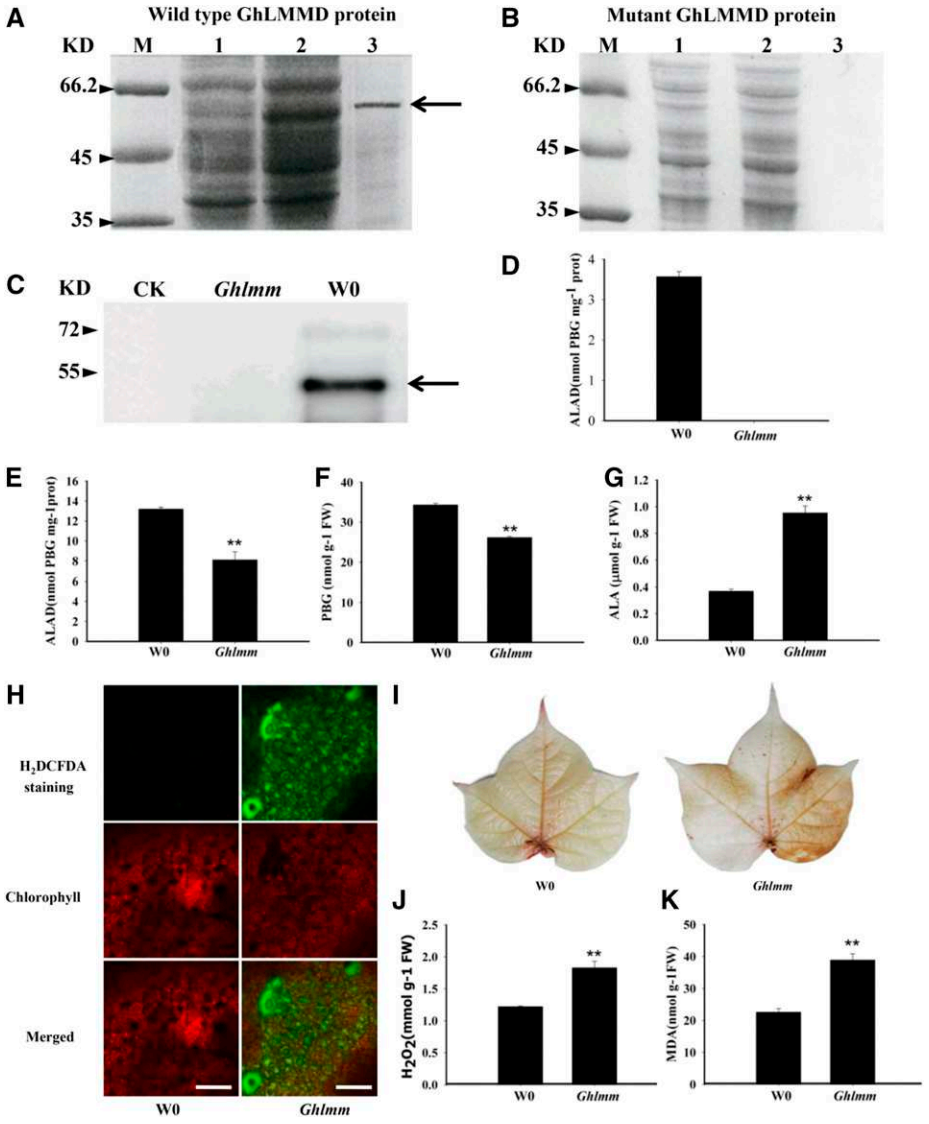

Figure 3. *GhLMMD* loss of function leads to accumulation of ALA and ROS burst. A and B, Expression and purification of wild-type and mutant GhLMMD proteins in *E. coli*. Lane M: protein marker; Lane 1: extracts from noninduced cells; Lane 2: extracts from IPTG-induced cells; Lane 3: GhLMMD protein purified from extracts of IPTG-induced *E. coli* cells. Arrow indicates the induced and purified GhLMMD protein, which is the same size with the predicted protein. Note that the wild-type GhLMMD protein could be expressed and purified from *E. coli*, while no mutant GhLMMD protein was expressed after induction. C, Confirmation of purified ALAD protein by western blotting. Antibodies against His-tag were used in the assay. CK, *Ghlmm*, and W0 indicate proteins purified from *E. coli* transformed with empty, mutant GhLMMD, and wild-type GhLMMD vector, respectively. D, ALAD enzyme activities of purified wild-type and mutant GhLMMD proteins. E, Analysis of ALAD enzyme activities in wild-type and mutant cotton leaves. F and G, Measurements of the contents of PBG and ALA in cotton leaves. Leaves of cotton seedlings at two-true-leaves stage were used for the analysis. H, Detection of ROS levels in cotton leaves by H_2DCFDA staining. Then 10 μM 2′,7′-dichlorodihydrofluorescein diacetate (H_2DCFD), a ROS-specific fluorescent indicator, was used for the staining. Bars = 50 μm. I, H_2O_2 visualization in cotton leaves by staining with DAB, showing more H_2O_2 was produced in the mutant than the wild type. J and K, Measurements of the contents of H_2O_2 and MDA in cotton leaves. Leaves of cotton seedlings at two-true-leaves stage were used for the analysis. At least three biological replicates were performed in each experiment. *$P < 0.05$ and **$P < 0.01$ (Student's *t* test).

The Lesion Mimic Mutants of Cotton Confer Resistance to *V. dahliae* Infection

As several lesion mimic mutants exhibit resistance to pathogen attacks, particularly to biotrophs (Mock and Grimm, 1997; Kruse et al., 1995; Molina et al., 1999; Tang et al., 2012; Wang et al., 2016), we investigated whether *Ghlmm* has acquired an elevated resistance to the *V. dahliae* infection. Infection assays showed that *Ghlmm* reached the resistance level of H7124, a resistant control for *V. dahlia* infection, while W0 was as susceptible as Jun1, a susceptible control for *V. dahliae*

infection. For instance, W0 and Jun1 showed significant wilting and etiolated leaves at 16 d postinoculation, but no obvious disease symptoms appeared in the leaves of *Ghlmm* and H7124 at this time point (Fig. 4A). At 28 d postinoculation, most W0 and Jun1 plants had died, the disease index of which was 79% and 92%, respectively. However, *Ghlmm* and H7124 showed fewer wilting and etiolated leaves, and the disease index was only 39% and 26%, respectively (Fig. 4, A and B). The resistance of *Ghlmm* to *V. dahliae* was further corroborated by the quantification of the fungal biomass in the leaves with q-PCR (Fig. 4C), microscopy of intensity of brown discoloration in stems (Supplemental Fig. S7A), and fungal recovery assays (Supplemental Fig. S7B).

Molecular Investigation for the Increased Resistance of the Mutant

To obtain comprehensive insights into the molecular basis for the increased resistance of *Ghlmm* to the *V. dahliae* infection, an RNA-seq was performed in *Ghlmm* and W0. The data revealed that a total of 2,069 differential expression genes ($q < 0.05$ and a fold change >2), with 1,541 up-regulated and 528 down-regulated genes, were detected in *Ghlmm* compared with W0. Gene ontology (GO) analysis of the biological processes showed that a subset of the genes belonging to response to stimulus (FDR = 1.7E-26), response to stress (FDR = 1.2E-21), response to biotic stimulus (FDR = 5.70E-10), response to chitin (FDR = 6.60E-08), defense response (FDR = 4.70E-05), and response to oxidative stress (FDR = 5.50E-05) were overrepresented in *Ghlmm*, indicating the defense-related pathway initiated in *Ghlmm* (Fig. 5A; Supplemental Table S4). Notably, 48 PR genes were significantly up-regulated in *Ghlmm*, ranging from a 4- to a 449-fold increase (Supplemental Table S5).

We have demonstrated that the ROS level is elevated in *Ghlmm*, and previous studies suggest that the ROS positively interplay with the SA. We thus measured the SA content in the roots, stems, and leaves of *Ghlmm* and W0. Although little was detected in roots, the SA levels significantly increased in the stems and leaves of *Ghlmm* compared with that in W0 plants (Fig. 5B). The SA signaling marker genes, such as the PR genes and

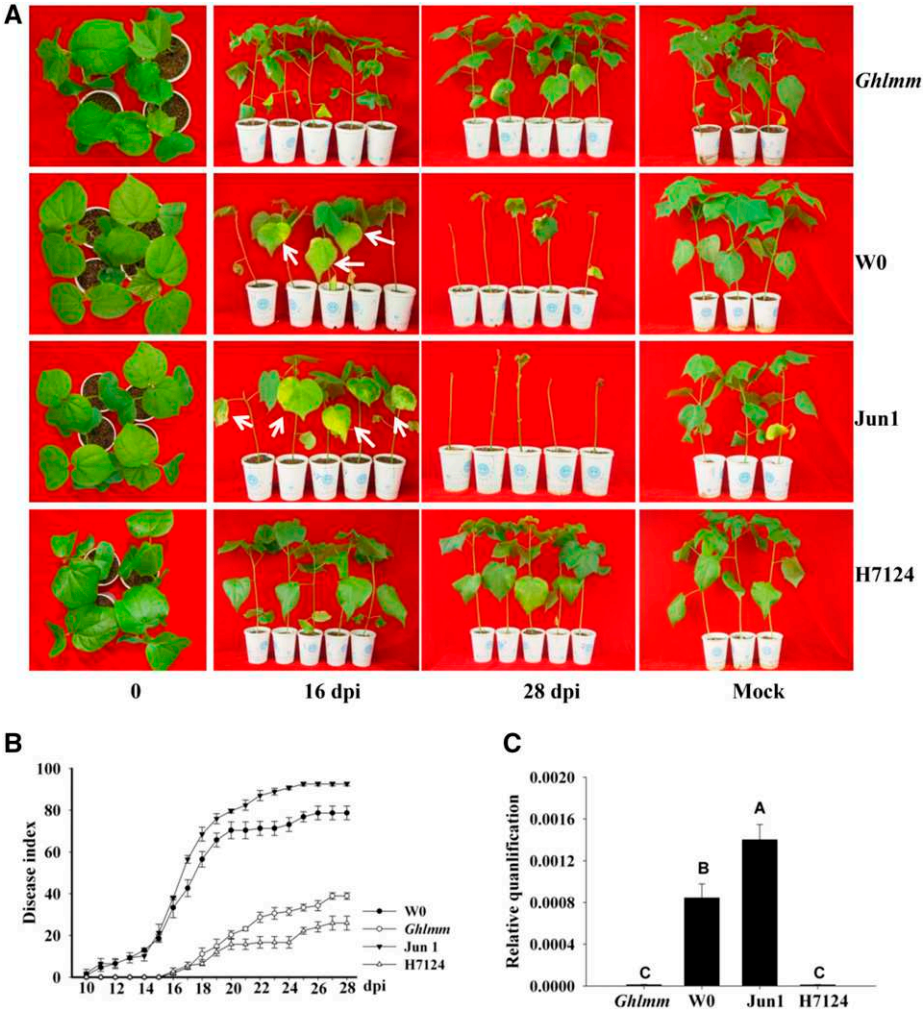

Figure 4. *Ghlmm* plants confers enhanced resistance to *V. dahliae* infection. A, Disease symptoms of *Ghlmm* compared with the wild-type W0, the susceptible control Jun1, and the resistant control H7124 challenged by *V. dahliae*. The mutant reached the resistance level of H7124. White arrows indicate disease symptoms on the leaves. B, The disease index of the mutants, W0, Jun1, and H7124. Error bars are SE calculated from three biological replicates, each containing 10 plants. C, qRT-PCR analysis of fungal biomass in leaves of the mutant and each of the controls. Different letters (A, B, C) indicate a statistically significant difference at $P < 0.01$ according to a randomization one-way ANOVA test. Error bars are SE of three biological replicates.

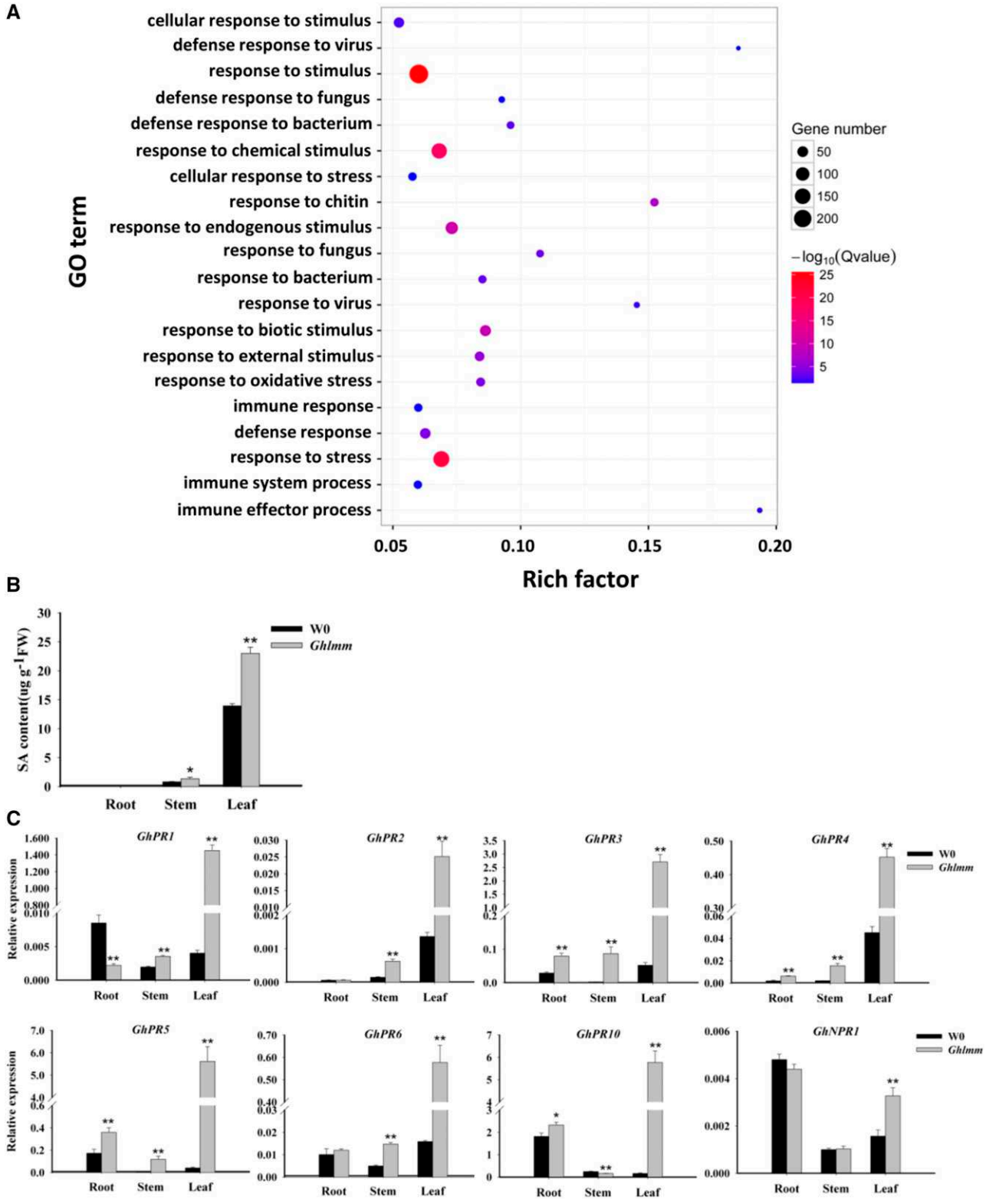

Figure 5. *Ghlmm* initiates immunity-related pathways and elevates SA accumulation and PR gene expression. A, GO enrichment analysis of the differentially expressed genes in leaves between *Ghlmm* and W0. The RNAs isolated from leaves of three individual plants were used for RNA-seq. *P* value of 0.05 adjusted by false discovery rate (FDR). Rich factor: percentage of enriched genes comparing with background in corresponding GO term. B, Measurement of SA content in different tissues of *Ghlmm* mutant and W0. The SA levels were significantly increased in leaves and stems of *Ghlmm* relative to the wild-type level. No SA

nonexpresser of PR genes 1 (*NPR1*), were significantly up-regulated in *Ghlmm*, particularly in the leaves and stems (Fig. 5C). The genes relating to the SA biosynthesis were also investigated by qRT-PCR. Expression of *EDS1* (enhanced disease susceptibility 1, encoding a lipase-like protein), *PAD4* (phytoalexin deficient 4, encoding a lipase-like protein), and *PAL* (encoding phenylalanine ammonia-lyase) was induced by H_2O_2 treatment in cotton leaves (Fig. 6A). Similarly, their expression was much higher in *Ghlmm* than in W0 (Fig. 6B). The enzyme activities of catalase (CAT), reported to be inhibited by SA, were drastically decreased in *Ghlmm* (Fig. 6C). Blocking SA biosynthesis pathway by application with 2-aminoindan-2-phosphonic acid (AIP), a highly specific inhibitor of PAL, significantly decreased levels of SA and ROS in both *Ghlmm* and W0 and eliminated the necrotic lesions in leaves of *Ghlmm* (Fig. 6, D and E). These data indicate that in cotton, the ROS positively interplay with the SA, and both contribute to the development of the lesion mimic phenotype and the resistance to *V. dahliae.* We also analyzed the PR gene expression in response to the SA levels. All PR genes tested were induced by the SA treatment in the wild-type cotton plants (Supplemental Fig. S8), similar to the constitutive expression levels in *Ghlmm*. On the contrary, blocking the SA biosynthesis pathway by application of the AIP suppressed the constitutive PR genes expression (except for PR2 and PR5) in *Ghlmm* to a similar level as in W0 (Supplemental Fig. S9).

The *GhLMM* Dosage Regulates the Degree of PCD, Defense Responses, and Resistance to *V. dahliae* Infection

Our previous experiments demonstrated that *GhLMM*-silenced wild-type plants show a more severe phenotype than the *Ghlmm* mutant, for example, exhibiting an arrest in the leaf development (Supplemental Fig. S4). This phenomenon prompted us to hypothesize that the expression level of *GhLMM* should be fine-tuned in plant cells, and perturbation of *GhLMM* expression level or changes in the *GhLMM* copies may lead to the aberration of cell growth and lesion mimic phenotype. To confirm the gene dosage-dependent response, we first started the experiments by regulating the endogenous ALAD enzyme activities in cotton leaves by spraying different concentrations of LA solution (ranging from 0 to 30 mM). After 24 h of treatment, the phenotype of the leaf, the PR gene expression, and several physiological parameters were investigated. The results showed that a 20-mM LA treatment could cause an evident lesion mimic phenotype, while a 0- to 10-mM LA treatment did not lead to visible leaf lesions (Fig. 7A). The increases in the PR gene expression and levels of ALA, H_2O_2, and SA were parallel correlated to the increased concentrations of the LA applied during treatment (Fig. 7, B and C). These results revealed that the levels of SA and H_2O_2, the defense-related gene expression, and the leaf lesions in cotton could be regulated by fine modulation of ALAD enzyme activity. Furthermore, we generated F_1 plants (containing one copy of the mutant gene, expressed as AADd) by crossing *Ghlmm* with W0. The F_1 and W0 plants were exposed to different concentrations of LA solution, respectively. Interestingly, the F_1 leaves exhibited evident lesions after 10 mM LA treatment, while visible cell death on W0 leaves appeared after 20 mM LA treatment (Supplemental Fig. S10A), indicating a dosage-dependent response to *GhLMM* copies in cotton. In addition, the phenotype of *GhLMM*-silenced plants in W0 and *Ghlmm* were characterized, respectively. The results showed that the *GhLMM*-silenced plants of both W0 and the mutant died, and no phenotypic difference could be observed (Supplemental Fig. S10, B and C).

We next explored the effects of the *GhLMM* gene dosage on disease resistance. The resistance of the F_1 plants to the *V. dahliae* infection was compared with *Ghlmm* and the wild-type cultivar W0. The results indicated that the resistance levels of these three lines were as follows: mutant $>$ F_1 $>$ wild type (Fig. 8, A and B). To support this, the expression level of *GhLMMD* in these lines was detected. *GhLMMD* expression in the F_1 plants was at midlevel between the parents, whereas no significant difference in the *GhLMMA* expression was detected between the parents and the F_1 plants (Fig. 9A). The enzyme activity of ALAD and CAT and the contents of ALA, PBG, H_2O_2, and SA in the F_1 plants were also at midlevel between the parents (Fig. 9, B and C). Similarly, the PR gene expression in these lines exhibited a gene dosage-dependent pattern (Fig. 9D).

To address whether the gene dosage-dependent resistance to *V. dahliae* works in a different genetic background, we crossed *Ghlmm* with two cotton cultivars, namely Jun1 and TM-1, respectively. The infection assays were performed with the F_1 plants and the parents from the two hybridization combinations. The results showed that the F_1 plants derived from the two hybridizations exhibited a similar resistance level (Supplemental Fig. S11) as the F_1 plants derived from the W0$\times$*Ghlmm* hybridization combination. Together, our genetic and molecular evidence demonstrated that the ALAD activity or the *GhLMM* gene copies in cotton may well correlate with the resistance to *V. dahliae* infections.

DISCUSSION

Ghlmm Is Caused by a Nonsense Mutation in ALAD Encoding Gene

We have identified a lesion mimic mutant named *Ghlmm* in cotton. To our knowledge, it is the first lesion

Figure 5. (*Continued.*)
could be detected in the roots. C, Transcription levels of PR and NPR1 genes in *Ghlmm* and W0 plants. All the tested genes were significantly up-regulated in leaves of *Ghlmm* plants compared with those in W0. $^{**}P < 0.01$ (Student's *t* test). Error bars are SE of three biological replicates.

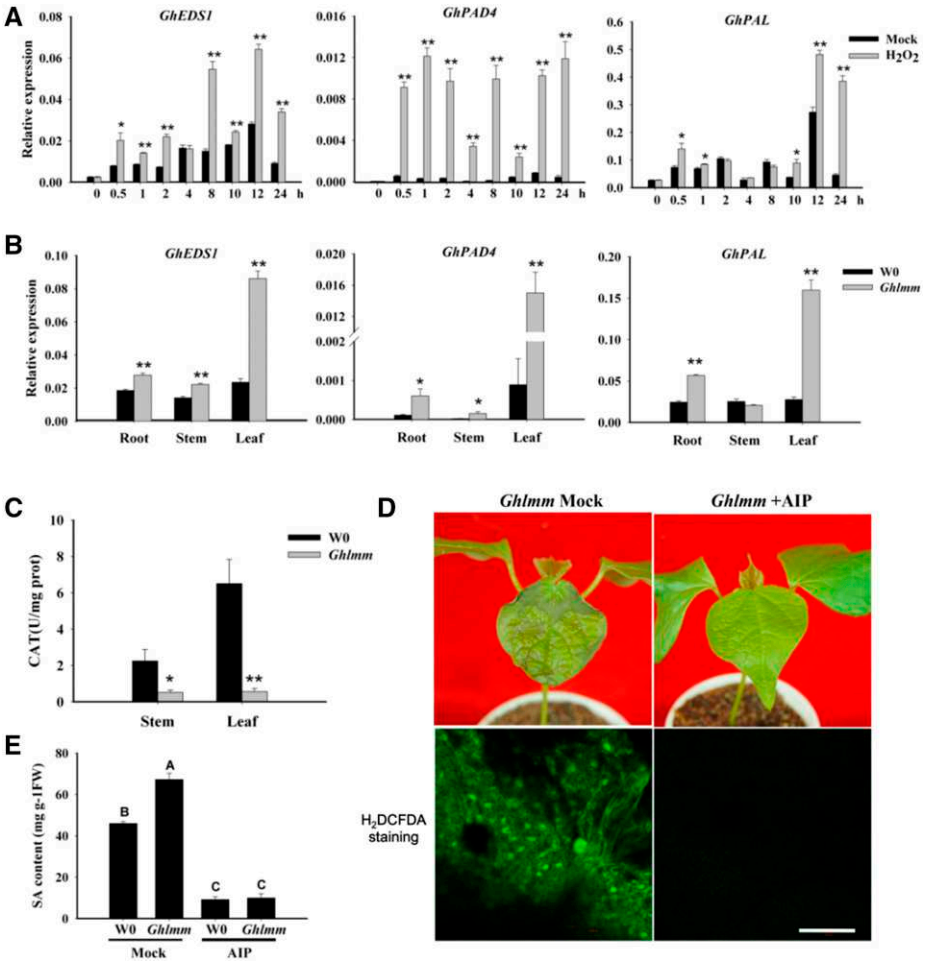

Figure 6. ROS production and SA biosynthesis form a self-amplifying feedback loop in *Ghlmm*. A, Expression of genes regulating to SA biosynthesis were induced by H_2O_2 treatment. The experiments were performed with the wild-type plants. *GhEDS1* and *GhPAD4* are genes positively regulating SA biosynthesis; *GhPAL* encodes a catalytic enzyme for SA biogenesis. B, *GhEDS1*, *GhPAD4*, and *GhPAL* were constitutively up-regulated in *Ghlmm* plants relative to W0. C, CAT (catalase, inhibited by SA) enzyme activity was significantly inhibited in leaves and stems of *Ghlmm* plants. D, Treatment with AIP, a SA biosynthesis inhibitor, reduced the ROS content and eliminated the cell death phenotype in *Ghlmm*. AIP is a highly specific inhibitor of PAL enzyme. Bars = 50 μm. E, After treatment with AIP, SA content in *Ghlmm* decreased to the wild-type level. At least three biological replicates were performed in each experiment. $^*P < 0.05$ and $^{**}P < 0.01$ (Student's *t* test). Different letters (A, B, C) indicate a statistically significant difference at $P < 0.01$ according to a randomization one-way ANOVA test. Error bars are SE of three biological replicates.

mimic mutant reported in cotton. Genetic and linkage analysis revealed that *Ghlmm* is controlled by a recessive nuclear gene located on chromosome D5. The gene responsible for the phenotype was cloned by a map-based strategy, indicating that it encodes the ALAD, a key enzyme in the tetrapyrrole biosynthesis pathway. In *Ghlmm* plants, a point mutation that resulted in pretermination was found in the coding region. Combined with the biochemical analysis of the wild-type and mutant GhLMMD proteins, we suppose that the mutant transcripts may be degraded more rapidly by nonsense mutation-mediated RNA surveillance system (Chang et al., 2007) and could not be translated into functional proteins. Therefore, the ALAD enzyme activity is lower in *Ghlmm*. We thus conclude that *Ghlmm* is a loss-of-function mutation derived from the wild-type gene.

Interestingly, *Gh_D05G2254*, another gene located in the same region of the *GhLMMD* locus, also showed significantly decreased expression in the mutant compared to wild-type plants (Fig S2). *Gh_D05G2254* encodes DNA lyase OGG1, which functions in oxidative stress-induced DNA demethylation. It has been shown that down-regulation of OGG1 may confer cells resistant to oxidative damage (Zhou et al., 2016). Here, down-regulation of this gene might be a downstream effect of overaccumulated ROS in the mutant.

Enzymes in the Tetrapyrrole Biosynthesis Pathway Might Be Tightly Controlled in Plants

The tetrapyrrole biosynthesis pathway is important in the production of four classes of tetrapyrroles, namely chlorophyll, heme, siroheme, and phytochromobilin in plants. Among them, chlorophyll plays key roles in photosynthesis by absorbing light and transferring the light energy or the electrons to other molecules. ALA, the universal precursor for tetrapyrrole synthesis, is converted to chlorophyll via sequential enzyme activities, with the first one being the ALAD. Analysis of the ALAD gene family from lower to higher plants revealed that very few ALAD gene members are present in plants ranging from algae to angiosperms (Fig. 2B), suggesting that ALAD gene copies or their expression levels are tightly controlled for cellular demand, as either defective or enhanced activity of ALAD can have detrimental effects on plant growth. In Arabidopsis, the overexpression of HEMB1 (encoding ALAD) in the wild type displayed photobleached leaves and did not survive,

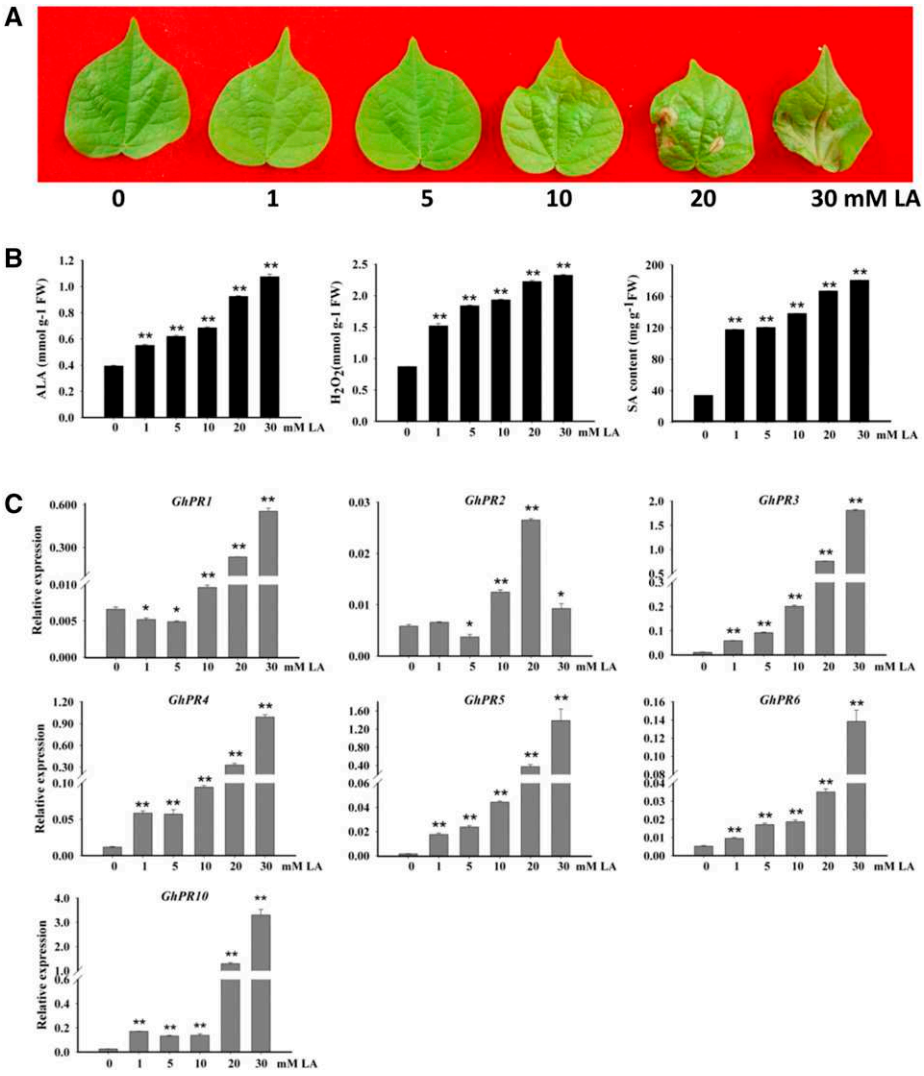

Figure 7. Mimic effects of *GhLMM* dosage on leaf phenotype by spraying LA. A, Leaf phenotype of W0 plants after being sprayed with different concentrations of LA solutions. Treatment with >20 mM LA solution leads to clear lesions on leaves. B, The content of ALA, H_2O_2, and SA was increased in W0 plants treated with different concentrations of LA solutions. C, PR gene expressions were up-regulated in W0 plants after LA treatment. At least three biological replicates were performed in each experiment. $*P < 0.05$ and $**P < 0.01$ (Student's *t* test).

and homozygotes hemb-1 mutants were also lethal (Tang et al., 2012). In our study, suppression of the ALAD in cotton leads to leaf growth arrest (Supplemental Fig. S4). In fact, most of the genes involved in tetrapyrrole biosynthesis in chloroplast might be precisely controlled in plants. Supporting information includes that (1) genes participating in tetrapyrrole biosynthesis, for example, *HEMA*, *HEMC*, *HEMD*, *HEME*, and *HEMF*, are only present in a few copy numbers in both Arabidopsis and *O. sativa* genomes (data not shown); and (2) antisense expression of *HEMA1* in Arabidopsis leads to a lethal phenotype (Kumar and Söll, 2000), and disruption of *HEMF1* caused plant growth alterations and the formation of necrotic lesions in leaves (Ishikawa et al., 2001; Sun et al., 2011).

ROS Derived from Chloroplast Could Enhance Plant Pathogen Resistance via SA-Dependent Pathway

In addition to the function of conducting photosynthesis in plants, chloroplast was recognized to play a central role in the defense response as the major steps of biosynthesis of defense hormones, such as SA, JA, and ABA, all occurred in chloroplast (Wildermuth et al., 2001; Wasternack and Hause, 2013; Serrano et al., 2016; Nambara and Marion-Poll, 2005). ROS has been implicated to play important roles in pathogen resistance (Shapiguzov et al., 2012). To date, most of the studies concentrate on the plant defense functions of apoplastic ROS, which was generated by plasma membrane respiratory burst oxidase homolog and cell wall peroxidase (Torres et al., 2005, 2006; Bolwell et al., 2002). Few studies provide convincing evidence that ROS produced in the chloroplast confers plant pathogen resistance. In this study, pretermination of *GhLMMD* decreased ALAD enzyme activity and resulted in the accumulation of ALA in chloroplast (Fig. 3, A-G). The accumulated ALA leads to relatively high levels of ROS via autoxidative decomposition (Fig. 3; Ryter and Tyrrell, 2000). ROS is proposed to act synergistically in a signal amplification loop with SA to induce the expression of PR genes and establishment of SAR

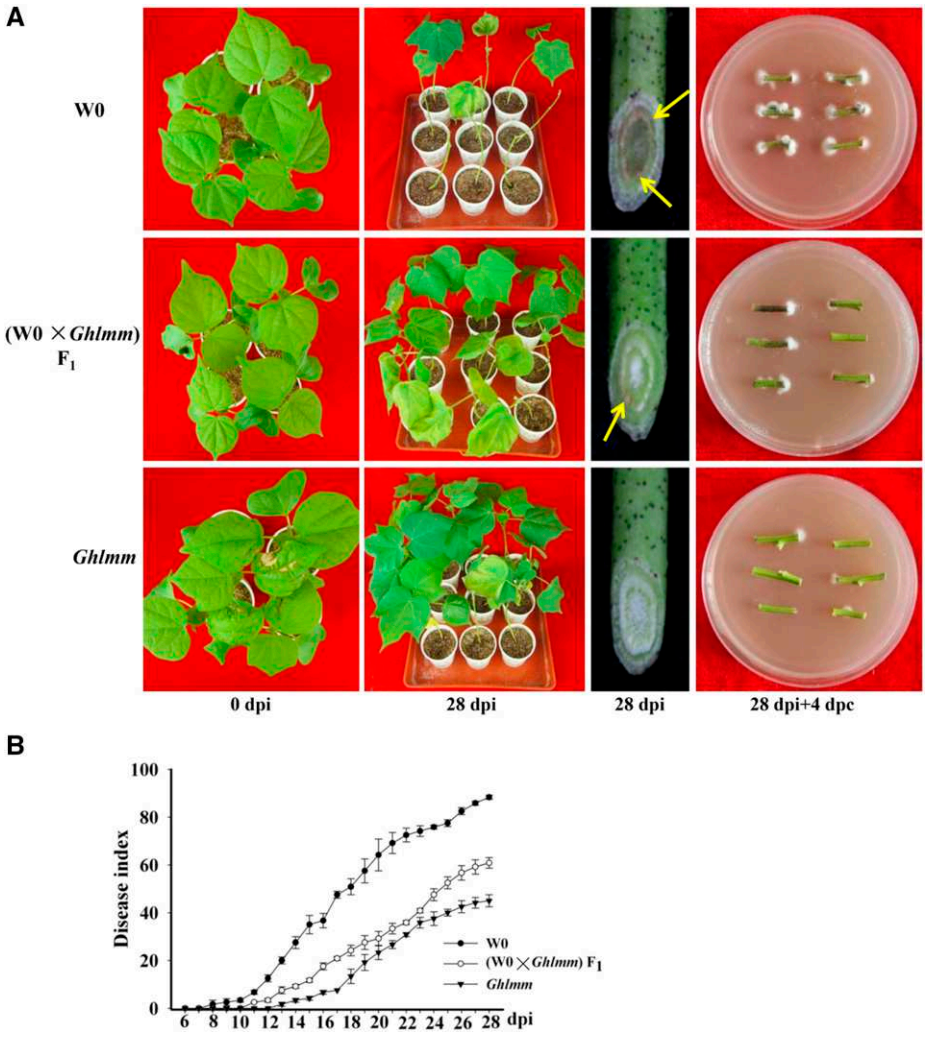

Figure 8. Disease resistance of *Ghlmm* plants and *GhLMM* dosage-dependent resistance to *V. dahliae* infection. A, Infection assays, visualization of fungal accumulation in stems, and fungal recovery experiments were performed to assess the disease resistance of indicated plant samples. The disease resistance of wild-type W0 (containing four copies of wild-type *GhLMM*, two copies of *GhLMMA* and *GhLMMD* each), the homozygote *Ghlmm* (containing two-copies of wild-type *GhLMMA* and two copies of mutant *GhLMMD*), and their F_1 plants (containing two copies of wild-type *GhLMMA*, one copy of wild-type *GhLMMD*, and one copy of mutant *GhLMMD*) to *V. dahliae* infection was evaluated. The severity of disease symptoms was as follows: W0 > F_1 > homozygote *Ghlmm*, exhibiting a dosage-dependent resistance to *V. dahliae* infection. The results from the fungal accumulation in stems and the fungal recovery experiments were similar to the infection assays. Each experiment has six biological replicates and repeated three times. Brown color indicated by arrows resulted from *V. dahliae* accumulation. DPC, days post culture. B, Disease index of W0, *Ghlmm*, and the F_1 plants. Error bars are SE calculated from three biological replicates each containing 10 plants.

(Dempsey et al., 1999). In our studies, SA biosynthesis positive regulating genes *EDS1*, *PAD4*, and *PAL* were significantly up-regulated in *Ghlmm* (Fig. 6B). On the other hand, CAT enzyme activity was inhibited in the mutant (Fig. 6C), which is consistent with previous findings that SA could inhibit CAT activity via binding its catalytic domain (Dempsey et al., 1999). Exogenous AIP (SA synthesis inhibitor) spraying on mutant leads to ROS scavenging. These results provide evidence for the self-amplifying feedback loop between ROS production and SA biosynthesis in plant. Produced ROS and induced SA could function as intercellular or intracellular second messengers to simultaneously mediate the establishment of HR, which induces PCD in plant cells, and SAR, which triggers defense-molecular production in the rest of the plant (Levine et al., 1994; Durrant and Dong, 2004).

Mutations in Essential Genes Will Not Lead to Lethality in Polyploidy Plants and Have Dosage Effect on Phenotype

To date, mutants misregulating in tetrapyrrole metabolism were discovered in diploid plants, such as Arabidopsis, maize, and rice, whereas no such research was reported in polyploidy plants including cotton. In contrast to the diploid plant species, polyploidy plants consist of more than one type of genome; they are derived from fusions between different diploid progenitors. For example, the allotetraploid cotton genome contains the A and D subgenomes, which originated from a single hybridization event between the A- and D- diploid species (Wendel, 1989). Gene redundancy and homologous genes are widely encountered in polyploidy plants, thus loss of function of a gene could be complemented by other genes with the same function and will probably not lead to visible phenotypic alterations. Thus, diploid plants could be vulnerable to genetic lesions, while polyploidy plants could be more resistant to most genetic defects. For example, mutation of *Les22* gene in diploid maize caused lethal phenotype (Hu et al., 1998). However, in this study, although ALAD genes were mutated on the D subgenome, the corresponding homologs on the A subgenome are normal in the mutant, and thus the cotton plants can still survive but display necrotic leaf damage, indicating

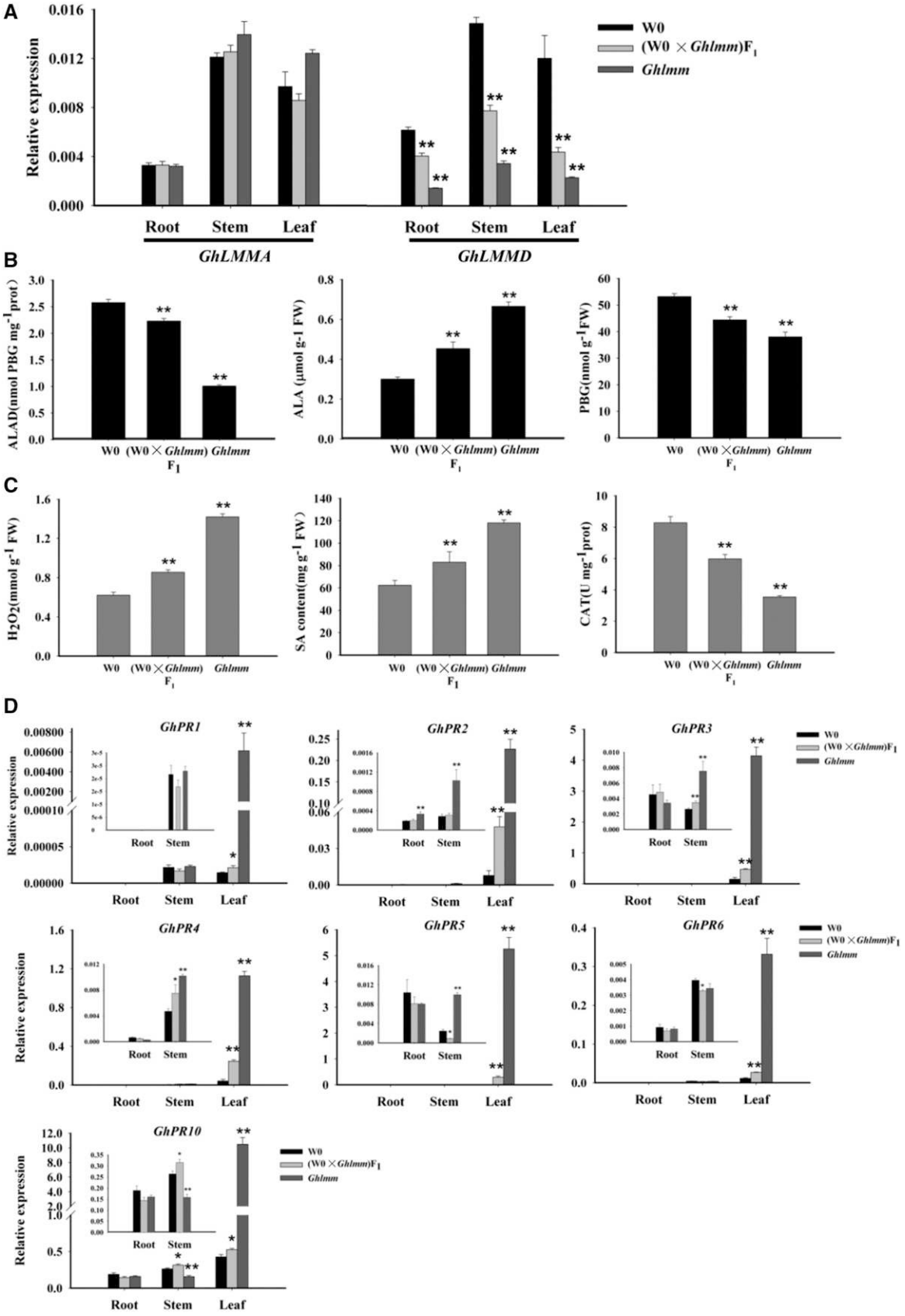

Figure 9. Molecular evidence of *GhLMM* dosage-dependent resistance to *V. dahliae* infection. A, Transcript abundance of *GhLMMA* and *GhLMMD* in different tissues of W0, *Ghlmm*, and the F_1 plants was analyzed by qRT-PCR using gene-specific primers. Expression of *GhLMMA* was not changed in the three lines. However, the expression of *GhLMMD* in the three lines was

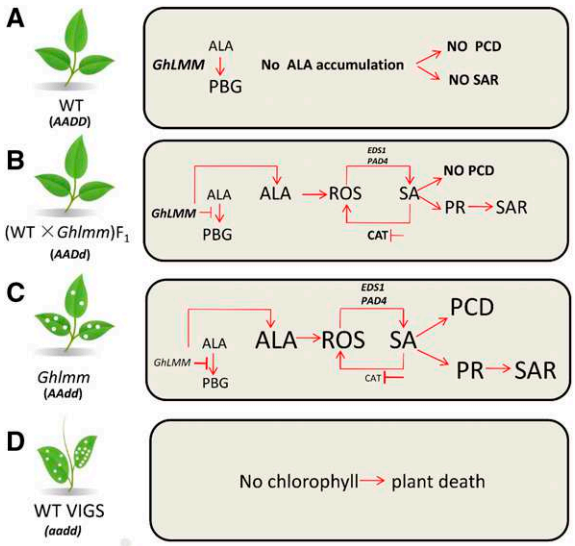

Figure 10. Proposed model of *GhLMM* dosage-dependent effects on the regulation of PCD and immunity. A, Four copies of *GhLMM* in tetraploid cotton (wild type, expressed as AADD) maintain the plants in normal growth without ALA accumulation and SAR activation. B, Three copies of *GhLMM* in cotton (F_1, expressed as AADd) leads to adequate ALA accumulation and proper degrees of ROS and SA levels and induction of SAR in the presence pathogen attack. Therefore, the plants exhibit no lesion on the leaves but have a high disease resistance level. C, Homozygous mutation with two copies of the mutant *GhLMMD* (*Ghlmm* mutant, expressed as AAdd) overaccumulate ALA, which might significantly increase the levels of ROS and SA, thus leading to disease lesion mimic phenotype on leaves in the absence of pathogen attack. D, Complete suppression of *GhLMM* by VIGS (expressed as aadd) results in no chlorophyll biosynthesis and eventually plant death. The body size in the figure denotes the content of corresponding molecules or degrees of signaling pathways involved. The bigger body size represents the more content of corresponding molecules or the higher degrees of signaling pathways.

higher tolerance to the genetic defects in polyploidy plants than in diploid plants.

To support the idea that the fine modulation of ALAD activity can affect the intensity of the PCD and the defense response, we used an ALAD inhibitor with a series of concentrations on cotton leaves and found that both the degree of PCD and the PR gene expressions are proportional to the increasing concentration of the inhibitor (Fig. 7). Further, *GhLMM* gene dosage-dependent leaf cell death was demonstrated via exposing W0 and F_1 plants to a range of LA solutions (Supplemental Figure S10A). These results indicated that the PCD and defense response can be tightly modulated by means of the fine regulation of ALAD activity. To investigate the effects of the ALAD gene dosage on cotton resistance to *V. dahliae*, we analyzed the resistance level of the homozygote mutant, the wild type, and their F_1 plants to the *V. dahliae* infection. As expected, the resistance levels of these lines are proportional to the copies of the mutant ALAD gene in the cotton genome (Fig. 8; Supplemental Figure S11). Similarly, in transgenic Arabidopsis plants expressing antisense *HEMA1* (encoding GluTR), different lines exhibiting varying degrees of chlorophyll deficiency were obtained, which displayed a range from a severe and intermediate to a negligible loss of chlorophyll (Kumar and Söll, 2000). These results reveal that the degree of mutant/lesion phenotypes could be tightly modulated by regulating the enzyme activity in steps of the tetrapyrrole biosynthesis pathway. Based on these results, we propose a model whereby the ALAD is involved in the regulation of PCD and innate immunity in allotetraploid cotton (Fig. 10). (1) Four copies of *GhLMM* maintain the plants in good conditions without ALA accumulation and defense activation. (2) Three copies exhibit no lesion on the leaves but lead to an increased level of ALA, ROS, and disease resistance. (3) Two copies display a significantly increased disease resistance level, but the lesion mimic phenotype occurs due to the ALA overaccumulation. (4) A simultaneous suppression of the *GhLMM* homeologs in tetraploid cotton blocks the tetrapyrrole and chlorophyll biosynthesis pathway and eventually leads to plant death. We suppose that a fine-tuning of ALAD activity between two and three copies might enhance the innate immunity without leaf cell death in tetraploid cotton. Moreover, as revealed by Kumar and Söll (2000), the traditional technique, the antisense method, might be superior to other techniques, such as the recently developed RNA interference and clustered regularly interspaced short palindromic repeats in modulating the ALAD gene expression due to a highly conserved sequence in the ALAD genes.

In this study, we found that mutation in the ALAD gene located on chromosome D5 of cotton confers enhanced resistance to *V. dahliae*. Although the mechanism requires a deep analysis at the molecular level, we suppose that the lesion mimic mutant we identified in cotton will have great potential applications in breeding cotton hybrid seeds with improved *V. dahliae* resistance. Furthermore, the *GhLMM* gene dosage effects can serve as an example that highlights the advantages of polyploidization in plants during evolution, with improving adaptation and elasticity to the environment.

Figure 9. (*Continued.*)
W0 > F_1 > *Ghlmm*, exhibiting a dosage-dependent expression pattern. B, ALAD enzyme activity, the content of ALA, PBG in W0, F_1, and *Ghlmm* cotton plant leaves. C, H_2O_2 and SA content were positively correlated with the *GhLMM* gene dosage, while CAT enzyme activity was negatively correlated with it. D, PR gene expressions in different tissues of W0, F_1, and *Ghlmm* showed a dosage-dependent expression pattern. Insets in the figures indicate the expression of corresponding genes in roots and stems. Error bars are SE calculated from five biological replicates. $^*P < 0.05$ and $^{**}P < 0.01$ (Student's *t* test).

MATERIALS AND METHODS

Plant Materials

Ghlmm, a lesion mimic mutant, was found in a screening of regenerated transgenic cotton plants, with *Gossypium hirsutum* L. acc. W0 as the wild-type receptor. TM-1 is a standard genetic line of Upland cotton. *G. hirsutum* cv Jun1 is highly susceptible to *Verticillium dahliae* infection and was used as the negative control. H7124 is a commercial *Gossypium barbadense* cultivar with high resistance to *V. dahliae* infection and was used as the positive control. The F_2 mapping population including 763 individuals was developed from a cross between TM-1 as the receptor parent and *Ghlmm* mutant as the donor parent. Three F_1 lines were generated from crosses between *Ghlmm* and W0, TM-1, and Jun1, respectively. All accessions were grown in the Jiangpu Experiment Station and in the green house under 28°C/24°C (day/night) and 16-h-light/8-h-dark cycle conditions. For temperature-dependent phenotypic assay, *Ghlmm* plants and the wild-type controls were grown at 23°C/20°C (day/night) for low-temperature conditions and 28°C/24°C (day/night) for high-temperature conditions on a 16-h-light/8-h-dark cycle; for light-dependent phenotypic assay, *Ghlmm* plants and the wild-type controls were grown in a plant room under 8-h-light/16-h-dark for short-day conditions and 16-h-light/8-h-dark cycle for long-day conditions. Fresh tissues used for a series of analysis, including DNA and RNA extraction, measurement of the levels of H_2O_2, ALA, PBG, SA, and enzyme activity, were collected and immediately frozen in liquid nitrogen and stored at −70°C until use.

Map-Based Cloning of the *GhLMMD* Gene

To map the gene responsible for the lesion mimic phenotype, an F_2 mapping population including 763 individuals was developed by a cross between *Ghlmm* and TM-1. Based on the previously published high-density tetraploid cotton linkage map (Guo et al., 2007) and the genome sequence of tetraploid cotton TM-1 (Zhang et al., 2015), the *GhLMMD* locus was preliminarily mapped between the molecular markers S2470 and S3184, with genetic distances of 4.1 and 15.9 cM respectively on Chr. D5. Furthermore, a microsatellite (SSR) marker NAU7928 and an SNP marker S2393 were developed, and the *GhLMMD* locus was narrowed to a 371-kb region. The cDNA and genomic DNA of the candidate genes within the region were amplified from W0, TM-1, and *Ghlmm* respectively, and the PCR products were confirmed by sequencing. All primers used in the study refer to Supplemental Table S2.

RNA Extraction and qRT-PCR

The total RNA was extracted from different tissues, including roots, stems, and leaves using the cetyltrimethyl ammonium bromide-acid phenol method (Shang et al., 2015). First-strand cDNA was generated using HiScript Q RT SuperMix for qPCR (+gDNA wiper) (Vazyme) according to the manufacturer's instructions. Real-time PCR was performed using a LightCycler FastStart DNA Master SYBR Green I kit (Roche) in a CFX96 Touch Real-Time PCR detection system (Bio-Rad, http://www.bio-rad.com). Three biological replicates were used for each analysis with three technical replicates each. The relative expression levels were calculated according to Livak and Schmittgen (Livak and Schmittgen, 2001). *GhLMM* subgenome-specific primers were designed based on the single nucleotide polymorphism between *GhLMMA* and *GhLMMD*. Other gene-specific primers were designed using Primer Premier 5. All primers are listed in Supplemental Table S2.

Subcellular Localization of *GhLMM*

The coding regions of *GhLMMA* and *GhLMMD* in W0 were fused with GFP in the pBinGFP4 vector to generate *pBin-35S::GhLMMA-GFP4* and *pBin-35S::GhLMMD-GFP4* respectively (Liu et al., 2014). The two vectors were transiently expressed in tobacco (*Nicotiana benthamiana*) leaf cells by *Agrobacterium tumefaciens* infiltration method (Liu et al., 2014). Vector (pt-rk-CD3-999)-containing chloroplast localized Rubisco protein labeled by mCherry was used as positive marker (Nelson et al., 2007). Subcellular localization of GhLMMA and GhLMMD was observed using a confocal laser scanning microscope (Zeiss LSM 780) at the specific excitation and emission wavelengths (GFP, 488 and 495–530 nm; mCherry, 587 and 600–650 nm).

Virus-Induced Gene Silencing Assay

A 412-bp fragment (corresponding to bases 585–996) of *GhLMMD* and a 417-bp fragment (corresponding to bases 73–489) of *Gh_05D2254* were cloned into pTRV2 (Gao et al., 2011), respectively, constructing the vectors named pTRV2: *GhLMMD* and pTRV2: *Gh_05D2254*. The two vectors and pTRV1 were introduced into the *Agrobacterium* strain GV3101 by means of the freeze-thawing method. The *Agrobacterium* strains containing pTRV2: *GhLMMD* and pTRV2: *Gh_05D2254* were respectively mixed with *Agrobacterium* strains containing pTRV1 at a ratio of 1:1. These mixtures were infiltrated in cotton cotyledons. More than 20 seedlings were used for each analysis. pTRV: *GhCLA1* was used as a control, and the silencing of *GhCLA1* produced the photobleaching phenotype. The plants were grown in pots at 23°C 20°C under a 16-h-light/8-h-dark cycle with 60% humidity. The primers used for the vector construction are listed in Supplemental Table S2. All VIGS assays were performed for three times independently.

Phylogenetic Analysis and Amino Acid Sequence Alignment of *ALAD* Orthologs in Plants

The *ALAD* genes were extracted from seventeen species, including algae, ferns, moss, gymnosperms, and angiosperms, to establish the phylogenetic tree. The genomic database of two sequenced cotton species, diploid *Gossypium arboreum* and tetraploid *G. hirsutum* acc. TM-1, was obtained from http://cgp.genomics.org.cn and http://mascotton.njau.edu.cn, respectively. The genomic database of *Picea abies* was obtained from http://congenie.org. The genomic database of other species was obtained from http://www.phytozome.net. The ALAD domain (Pfam00490) seed file was downloaded from http://pfam.janelia.org and used as the query to individually scan the protein databases with the HMMER software (version 3.0; Eddy, 2011). All the identified ALAD proteins were aligned with the Clustal W program. MEGA 5.0 software (www.megasoftware.net) was used for constructing the phylogenetic tree using the JTT model in the maximum-likelihood method, and the bootstrap value was set at 1,000. The Clustal X software (http://www.clustal.org/) was used for amino acid sequence alignment of ALAD proteins from rice (*Oryza sativa*), Arabidopsis (*Arabidopsis thaliana*), *Theobroma cacao*, and *G. hirsutum*, respectively. The Genedoc software (http://www.nrbsc.org/gfx/genedoc/ebinet.htm) was used for visualizing the result.

Recombinant Protein Expression and Purification

The encoding region of the wild-type *GhLMMD* and its corresponding mutant gene were cloned into the *Bam*HI sites in a pET-28a vector using the ClonExpress II One Step Cloning Kit (Vazyme, C112-01), resulting in a translational fusion of the wild type and the mutant protein with six His residues at the N- and C- terminus, respectively. The plasmids were transformed into *Escherichia coli* BL21 (DE3). The positive clones were grown at 37°C in LB medium with 50 mg L^{-1} kanamycin to an OD_{600} of 0.8. Expression of fusion protein was induced by addition of 1 mM isopropylthio-β-galactoside (IPTG) and growth at 16°C for 16 h. Cells were suspended in buffer (0.05 M Tris-HCl, 0.1 mM dithiothreitol, 6 M urea, pH 8.2) and broken by ultrasonic method. The proteins were purified using a Ni-NTA column (Qiagen). After denaturing in urea and gradient dialysis, refolded GhLMMD protein was obtained and then used for enzyme activity assay, SDS-PAGE analysis, and western blotting. HRP-conjugated anti-His antibody (Proteintech) was used in western blotting as described (Bu et al., 2017).

Measurement of the Levels of ALA and PBG and the Enzyme Activity of ALAD

The ALA content was measured according to Mauzerall and Granick (1956). In brief, frozen samples were homogenized and suspended in a 500-μL 20 mM potassium phosphate buffer (pH 6.8). The samples were then centrifuged for 10 min at 12,000 rpm at 4°C. Then 400 μL of supernatant was transferred to a new tube and mixed with 100 μL ethyl-acetoacetate. After boiling for 10 min at 100°C, it was mixed with 500 μL of Ehrlich's reagent for 5 min, and then the absorption was measured at 553 nm. The ALA content of the samples was calculated using the standard curve generated by the commercial ALA.

The PBG content measurement was performed as described by Kayser et al. (2005). ALAD enzyme activity was determined using the methods described by Vajpayee et al. (2000) with the buffer (0.16 mg/mL ALA, 40 mM Tris-HCl, 80 mM

dithiothreitol, 9.4 mM $MgCl_2$, pH 8.2), expressed as nmol PBG/per milligram protein per hour at 37°C.

Evaluation of the Resistance to *V. dahliae* Invasion

For assessment of *Verticillium* wilt resistance, cotton seeds were grown in pots with a mixture of peat and vermiculite (1:1, v/v). The defoliating *V. dahliae* isolate 'V991' was grown on potato dextrose agar at 25°C for 4 d. Then, mycelia were collected and cultured in liquid Czapek's medium for 5 d. Cotton seedlings at two true-leaf stages were inoculated with V991 by soil drenching with 20 mL spore suspensions (10^7 conidia/mL). The disease index was calculated using the following formula: disease index = [($\sum$disease grades × number of infected plants)/ (total checked plants×4)] ×100. Each experiment group included at least 10 individual plants and was repeated three times. Mock inoculated plants were used as negative controls.

To quantify the fungal biomass in cotton leaves, the first true leaves of the cotton plants inoculated with V991 were collected for DNA extraction. The amounts of fungal DNA were quantified by calculating the products of the ITS1 and ITS2 regions of the rRNA genes (Z29511) of *V. dahliae* relative to the products of cotton histone gene (AF024716; Zhang et al., 2016). Fungal accumulation was also demonstrated by microscopy based on the intensity of the brown stem discoloration resulting from the fungi accumulation. To do this, stems were collected at the position of 1 cm above the cotyledons knot at 16 d after inoculation, free-hand sectioned, and observed using a microscope.

For fungal recovery assay, stems and leaves were surface sterilized for 1 min in 70% ethanol, rinsed with sterile water 8 times, and then sliced into sections. The stem and leaf sections were placed on the potato dextrose agar supplemented with chloramphenicol (34 mg L^{-1}) and cultured for 4 d at 25°C, then photographed.

Detection and Measurement of the Levels of ROS, H_2O_2, MDA, and CAT Enzyme Activity

The ROS generation in the cotton leaf was examined with H_2DCFDA staining. Cotton leaves were washed with sterile water and incubated in 10 μM H_2DCFDA for 30 min in dark at 30°C. The samples were then washed with sterile water 3 times, and the staining signals were observed using a microscope.

To visualize the accumulation of H_2O_2, fresh cotton leaves were collected, incubated in a DAB solution (1 mg/mL, pH 3.8) for 8 h, and then decolorized in 96% ethanol. The quantification of H_2O_2 in leaves was performed with a commercial H_2O_2 detection kit (Jiancheng Bioengineering Institute).

The MDA content in leaves was measured with a commercial plant MDA detection kit (Jiancheng Bioengineering Institute). The CAT enzyme activity in leaves was determined with a CAT detection kit (Jiancheng Bioengineering Institute).

Salicylic Acid Measurement

The SA was measured according to the method described by Verberne et al. with minor modifications (Verberne et al., 2002). In brief, the cotton leaves were collected and ground in liquid nitrogen. Then, the samples were mixed with 90% methanol and centrifuged. After collecting the supernatant, the pellet was suspended in 100% methanol and centrifuged again. The supernatants were combined and added with 10 μL 0.2 M sodium hydroxide and then evaporated in a SpeedVac concentrator. The residues were resuspended in 5% trichloroacetic acid. The solutions were extracted twice with a 800-μL mixture of ethyl-acetate:cyclohexane (1:1). The upper organic phases were collected. The lower trichloroacetic acid phase was acid hydrolyzed with 300 μL 8 M hydrochloric acid (1 h, 80°C) and was extracted twice with 800 μL ethyl-acetate:cyclohexane (1:1). The organic phases were collected, combined with the above organic phase solutions, then added with 120 μL 0.2 M sodium acetate and evaporated in a SpeedVac concentrator. The residues were dissolved in 900 μL methanol, and the SA content was analyzed by HPLC and calculated according to the standard SA curve that was made from commercial SA purchased from Sigma.

Treatment of Plants with AIP and LA

AIP, the highly specific inhibitor for the PAL enzyme that catalyzes the SA biogenesis, was used to block the biosynthesis of SA. Ten days after sowing, the cotton seedlings with visible true leaves were treated with AIP at a concentration of 1 mM. The control plants were treated with sterile water. The AIP or mock treated cotton leaves were collected when the *Ghlmm* mutant exhibited the necrotic lesion phenotype. Fresh leaves were used for the ROS observation.

For the LA treatment, cotton plants were grown up to the two-true-leaves stage for about 16 d after sowing. Different concentrations of the LA solutions were sprayed on the leaves of the cotton seedlings. Twenty-four hours after spraying, the leaves were collected for use.

Transcriptome Sequencing

The leaves of *Ghlmm* and W0 were collected 15 d after sowing, and the total RNA of the leaves was extracted by means of the cetyltrimethyl ammonium bromide-sour phenol extraction method (Jiang and Zhang, 2003). Sequencing was performed on the Illumina HiSeq2000 platform. After preprocessing the RNA-seq data with an NGS QC toolkit (Patel and Jain, 2012), the reads were mapped to the *G. hirsutum* TM-1 genome using a Tophat spliced aligner with default parameters (Trapnell et al., 2009). The genome-matched reads from each library were assembled with Cufflinks (Trapnell et al., 2012). Cuffmerge was then used to merge the individual transcript assemblies into a single transcript set. Lastly, Cuffdiff was used to find differentially expressed genes with a cutoff of 0.05 q value and a fold change of >2. The GO analysis of the differentially expressed genes in the biological process was conducted using the AgriGO software (Du et al., 2010). The input sample list was the Arabidopsis gene ID, which was converted from the Upland cotton gene ID (http://genome.jgi.doe.gov/) and the background was constituted by the whole annotated genes in Arabidopsis. The output of enrichment needed FDR < 0.05.

Accession Numbers

All sequence files are available at DDBJ/EMBL/GenBank under the accession numbers KY652847 (*GhLMMA* of *G. hirsutum* acc. TM-1), KY652848 (*GhLMMD* of *G. hirsutum* acc. TM-1), KY652849 (*GhLMMA* of *G. hirsutum* acc. W0), and KY652850 (*GhLMMD* of *G. hirsutum* acc. W0). Transcriptome data have been deposited in GenBank under the accession number PRJNA369440.

Supplemental Data

The following supplemental materials are available.

Supplemental Figure S1. *Ghlmm* mutant develops lesions on leaves in a temperature- and light-dependent manner.

Supplemental Figure S2. Expression pattern of candidate genes in leaves of TM-1, W0, and *Ghlmm* mutant.

Supplemental Figure S3. *Gh_D05G2254* is not the causative gene responsible for *Ghlmm* phenotype.

Supplemental Figure S4. Functional characterization of *GhLMM* (*Gh_D05G2237*) by VIGS analysis.

Supplemental Figure S5. Amino acid sequence alignment of ALAD proteins.

Supplemental Figure S6. LA spraying leads to *Ghlmm* phenotype and accumulation of ALA and H_2O_2 in wild-type W0.

Supplemental Figure S7. *V. dahliae* content was significantly reduced in *Ghlmm* stems and leaves.

Supplemental Figure S8. The PR genes were induced by SA treatment.

Supplemental Figure S9. Expression of most PR genes in *Ghlmm* mutant was down-regulated to the same levels as those in W0 after AIP treatment.

Supplemental Figure S10. The effects of *GhLMM* dosage on leaf phenotype.

Supplemental Figure S11. Effects of *GhLMM* mutation on resistance to *V. dahliae* infection under different genetic backgrounds.

Supplemental Table S1. Fiber qualities and seed parameters in *Ghlmm* and W0.

Supplemental Table S2. All primers used in this study.

Supplemental Table S3. Information of ALAD genes from *Gossypium*, Arabidopsis, and other species.

Supplemental Table S4. GO analysis involved in biological processes.

Supplemental Table S5. PR genes significantly upregulated in *Ghlmm*.

ACKNOWLEDGMENTS

This work was supported by National Key R & D Program for Crop Breeding (2016YFD0100306) and Jiangsu Collaborative Innovation Center for Modern Crop Production project (No. 10). The funders had no role in study design, data collection and analysis, decision to publish, or preparation of the manuscript.

Received June 20, 2017; accepted July 20, 2017; published July 27, 2017.

LITERATURE CITED

Balagué C, Lin B, Alcon C, Flottes G, Malmström S, Köhler C, Neuhaus G, Pelletier G, Gaymard F, Roby D (2003) HLM1, an essential signaling component in the hypersensitive response, is a member of the cyclic nucleotide-gated channel ion channel family. Plant Cell **15:** 365–379

Bolwell GP, Bindschedler LV, Blee KA, Butt VS, Davies DR, Gardner SL, Gerrish C, Minibayeva F (2002) The apoplastic oxidative burst in response to biotic stress in plants: a three-component system. J Exp Bot **53:** 1367–1376

Brodersen P, Petersen M, Pike HM, Olszak B, Skov S, Odum N, Jørgensen LB, Brown RE, Mundy J (2002) Knockout of *Arabidopsis* accelerated-cell-death11 encoding a sphingosine transfer protein causes activation of programmed cell death and defense. Genes Dev **16:** 490–502

Bruggeman Q, Raynaud C, Benhamed M, Delarue M (2015) To die or not to die? Lessons from lesion mimic mutants. Front Plant Sci **6:** 24

Bu W, Liang Q, Zhi L, Maciunas L, Loll PJ, Eckenhoff RG, Covarrubias M (2017) Sites and functional consequence of alkylphenol anesthetic binding to Kv1.2 channels. Mol Neurobiol 10.1007/s12035-017-0437-2

Büschges R, Hollricher K, Panstruga R, Simons G, Wolter M, Frijters A, van Daelen R, van der Lee T, Diergaarde P, Groenendijk J, et al (1997) The barley Mlo gene: a novel control element of plant pathogen resistance. Cell **88:** 695–705

Chang YF, Imam JS, Wilkinson MF (2007) The nonsense-mediated decay RNA surveillance pathway. Annu Rev Biochem **76:** 51–74

Dempsey DA, Shah J, Klessig DF (1999) Salicylic acid and disease resistance in plants. CRC Crit Rev Plant Sci **18:** 547–575

Dietrich RA, Richberg MH, Schmidt R, Dean C, Dangl JL (1997) A novel zinc finger protein is encoded by the Arabidopsis LSD1 gene and functions as a negative regulator of plant cell death. Cell **88:** 685–694

Du Z, Zhou X, Ling Y, Zhang Z, Su Z (2010) agriGO: a GO analysis toolkit for the agricultural community. Nucleic Acids Res **38:** W64–70

Durrant WE, Dong X (2004) Systemic acquired resistance. Annu Rev Phytopathol **42:** 185–209

Eddy SR (2011) Accelerated profile HMM searches. PLOS Comput Biol **7:** e1002195

Gao X, Wheeler T, Li Z, Kenerley CM, He P, Shan L (2011) Silencing *GhNDR1* and *GhMKK2* compromises cotton resistance to *Verticillium wilt*. Plant J **66:** 293–305

Guo W, Cai C, Wang C, Han Z, Song X, Wang K, Niu X, Wang C, Lu K, Shi B, et al (2007) A microsatellite-based, gene-rich linkage map reveals genome structure, function and evolution in Gossypium. Genetics **176:** 527–541

Heath MC (2000) Hypersensitive response-related death. Plant Mol Biol **44:** 321–334

Hu G, Yalpani N, Briggs SP, Johal GS (1998) A porphyrin pathway impairment is responsible for the phenotype of a dominant disease lesion mimic mutant of maize. Plant Cell **10:** 1095–1105

Ishikawa A, Okamoto H, Iwasaki Y, Asahi T (2001) A deficiency of coproporphyrinogen III oxidase causes lesion formation in *Arabidopsis*. Plant J **27:** 89–99

Jiang J, Zhang T (2003) Extraction of Total RNA in Cotton Tissues with CTAB-acidic Phenolic Method. Cotton Sci **15:** 166–167

Kachroo P, Shanklin J, Shah J, Whittle EJ, Klessig DF (2001) A fatty acid desaturase modulates the activation of defense signaling pathways in plants. Proc Natl Acad Sci USA **98:** 9448–9453

Kayser H, Krull-Savage U, Rilk-van Gessel R (2005) Developmental profiles of 5-aminolevulinate, porphobilinogen and porphobilinogen synthase activity in Pieris brassicae related to the synthesis of the bilin-binding protein. Insect Biochem Mol Biol **35:** 165–174

Kruse E, Mock HP, Grimm B (1995) Reduction of coproporphyrinogen oxidase level by antisense RNA synthesis leads to deregulated gene expression of plastid proteins and affects the oxidative defense system. EMBO J **14:** 3712–3720

Kumar AM, Söll D (2000) Antisense HEMA1 RNA expression inhibits heme and chlorophyll biosynthesis in *arabidopsis*. Plant Physiol **122:** 49–56

Levine A, Tenhaken R, Dixon R, Lamb C (1994) H_2O_2 from the oxidative burst orchestrates the plant hypersensitive disease resistance response. Cell **79:** 583–593

Liu T, Song T, Zhang X, Yuan H, Su L, Li W, Xu J, Liu S, Chen L, Chen T, et al (2014) Unconventionally secreted effectors of two filamentous pathogens target plant salicylate biosynthesis. Nat Commun **5:** 4686

Livak KJ, Schmittgen TD (2001) Analysis of relative gene expression data using real-time quantitative PCR and the 2(-Delta Delta C(T)) method. Methods **25:** 402–408

Mauzerall D, Granick S (1956) The occurrence and determination of delta-amino-levulinic acid and porphobilinogen in urine. J Biol Chem **219:** 435–446

Mock HP, Grimm B (1997) Reduction of uroporphyrinogen decarboxylase by antisense RNA expression affects activities of other enzymes involved in tetrapyrrole biosynthesis and leads to light-dependent necrosis. Plant Physiol **113:** 1101–1112

Molina A, Volrath S, Guyer D, Maleck K, Ryals J, Ward E (1999) Inhibition of protoporphyrinogen oxidase expression in *Arabidopsis* causes a lesion-mimic phenotype that induces systemic acquired resistance. Plant J **17:** 667–678

Nambara E, Marion-Poll A (2005) Abscisic acid biosynthesis and catabolism. Annu Rev Plant Biol **56:** 165–185

Nelson BK, Cai X, Nebenfuhr A (2007) A multicolored set of in vivo organelle markers for co-localization studies in *Arabidopsis* and other plants. Plant J **51:** 1126–1136

Patel RK, Jain M (2012) NGS QC Toolkit: a toolkit for quality control of next generation sequencing data. PLoS One **7:** e30619

Pennell RI, Lamb C (1997) Programmed cell death in plants. Plant Cell **9:** 1157–1168

Quesada V, Sarmiento-Mañús R, González-Bayón R, Hricová A, Ponce MR, Micol JL (2013) PORPHOBILINOGEN DEAMINASE deficiency alters vegetative and reproductive development and causes lesions in *Arabidopsis*. PLoS One **8:** e53378

Ryter SW, Tyrrell RM (2000) The heme synthesis and degradation pathways: role in oxidant sensitivity. Heme oxygenase has both pro- and antioxidant properties. Free Radic Biol Med **28:** 289–309

Serrano I, Audran C, Rivas S (2016) Chloroplasts at work during plant innate immunity. J Exp Bot **67:** 3845–3854

Shang X, Chai Q, Zhang Q, Jiang J, Zhang T, Guo W, Ruan YL (2015) Down-regulation of the cotton endo-1,4-β-glucanase gene KOR1 disrupts endosperm cellularization, delays embryo development, and reduces early seedling vigour. J Exp Bot **66:** 3071–3083

Shapiguzov A, Vainonen JP, Wrzaczek M, Kangasjärvi J (2012) ROS-talk - how the apoplast, the chloroplast, and the nucleus get the message through. Front Plant Sci **3:** 292

Shirasu K, Schulze-Lefert P (2000) Regulators of cell death in disease resistance. Plant Mol Biol **44:** 371–385

Sun C, Liu L, Tang J, Lin A, Zhang F, Fang J, Zhang G, Chu C (2011) RLIN1, encoding a putative coproporphyrinogen III oxidase, is involved in lesion initiation in rice. J Genet Genomics **38:** 29–37

Tang W, Wang W, Chen D, Ji Q, Jing Y, Wang H, Lin R (2012) Transposase-derived proteins FHY3/FAR1 interact with PHYTOCHROME-INTERACTING FACTOR1 to regulate chlorophyll biosynthesis by modulating HEMB1 during deetiolation in *Arabidopsis*. Plant Cell **24:** 1984–2000

Torres MA, Jones JDG, Dangl JL (2005) Pathogen-induced, NADPH oxidase-derived reactive oxygen intermediates suppress spread of cell death in Arabidopsis thaliana. Nat Genet **37:** 1130–1134

Torres MA, Jones JD, Dangl JL (2006) Reactive oxygen species signaling in response to pathogens. Plant Physiol **141:** 373–378

Trapnell C, Pachter L, Salzberg SL (2009) TopHat: discovering splice junctions with RNA-Seq. Bioinformatics **25:** 1105–1111

Trapnell C, Roberts A, Goff L, Pertea G, Kim D, Kelley DR, Pimentel H, Salzberg SL, Rinn JL, Pachter L (2012) Differential gene and transcript expression analysis of RNA-seq experiments with TopHat and Cufflinks. Nat Protoc **7:** 562–578

Vajpayee P, Tripathi RD, Rai UN, Ali MB, Singh SN (2000) Chromium (VI) accumulation reduces chlorophyll biosynthesis, nitrate reductase activity and protein content in *Nymphaea alba L.* Chemosphere **41:** 1075–1082

Vaux DL, Korsmeyer SJ (1999) Cell death in development. Cell **96:** 245–254

Verberne MC, Brouwer N, Delbianco F, Linthorst HJ, Bol JF, Verpoorte R (2002) Method for the extraction of the volatile compound salicylic acid from tobacco leaf material. Phytochem Anal **13:** 45–50

Wang F, Wu W, Wang D, Yang W, Sun J, Liu D, Zhang A, Yang W, Sun J, Liu D, et al (2016) Characterization and genetic analysis of a novel light dependent lesion mimic mutant, lm3, showing adult-plant resistance to powdery mildew in common wheat. PLoS One **11:** e0155358

Wang W, Tang W, Ma T, Niu D, Jin JB, Wang H, Lin R (2015) A pair of light signaling factors FHY3 and FAR1 regulates plant immunity by modulating chlorophyll biosynthesis. J Integr Plant Biol **58:** 91–103

Wasternack C, Hause B (2013) Jasmonates: biosynthesis, perception, signal transduction and action in plant stress response, growth and development. An update to the 2007 review in Annals of Botany. Ann Bot (Lond) **111:** 1021–1058

Wendel JF (1989) New World tetraploid cottons contain Old World cytoplasm. Proc Natl Acad Sci USA **86:** 4132–4136

Wildermuth MC, Dewdney J, Wu G, Ausubel FM (2001) Isochorismate synthase is required to synthesize salicylic acid for plant defence. Nature **414:** 562–565

Zhang T, Hu Y, Jiang W, Fang L, Guan X, Chen J, Zhang J, Saski CA, Scheffler BE, Stelly DM, et al (2015) Sequencing of allotetraploid cotton (*Gossypium hirsutum L.* acc. TM-1) provides a resource for fiber improvement. Nat Biotechnol **33:** 531–537

Zhang Z, Zhao J, Ding L, Zou L, Li Y, Chen G, Zhang T (2016) Constitutive expression of a novel antimicrobial protein, Hcm1, confers resistance to both *Verticillium* and *Fusarium wilts* in cotton. Sci Rep **6:** 20773

Zhou X, Zhuang Z, Wang W, He L, Wu H, Cao Y, Pan F, Zhao J, Hu Z, Sekhar C, et al (2016) OGG1 is essential in oxidative stress induced DNA demethylation. Cell Signal **28:** 1163–1171